NATIONAL ADVISORY COMMITTEE FOR AERONAUTICS

REPORT No. 592

FULL-SCALE TESTS OF N. A. C. A. COWLINGS

By THEODORE THEODORSEN, M. J. BREVOORT
and GEORGE W. STICKLE

1937

For sale by the Superintendent of Documents, Washington, D. C. - - - - - - - - - - - - - - Price 15 cents
Subscription price $3 per year

AERONAUTIC SYMBOLS

1. FUNDAMENTAL AND DERIVED UNITS

	Symbol	Metric		English	
		Unit	Abbreviation	Unit	Abbreviation
Length	l	meter	m	foot (or mile)	ft. (or mi.)
Time	t	second	s	second (or hour)	sec. (or hr.)
Force	F	weight of 1 kilogram	kg	weight of 1 pound	lb.
Power	P	horsepower (metric)		horsepower	hp.
Speed	V	kilometers per hour	k.p.h.	miles per hour	m.p.h.
		meters per second	m.p.s.	feet per second	f.p.s.

2. GENERAL SYMBOLS

W, Weight$=mg$

g, Standard acceleration of gravity$=9.80665$ m/s^2 or 32.1740 ft./sec.^{2}

m, Mass$=\frac{W}{g}$

I, Moment of inertia$=mk^2$. (Indicate axis of radius of gyration k by proper subscript.)

μ, Coefficient of viscosity

ν, Kinematic viscosity

ρ, Density (mass per unit volume)

Standard density of dry air, 0.12497 kg-m^{-4}-s^2 at 15° C. and 760 mm; or 0.002378 lb.-ft.$^{-4}$ sec.^{2}

Specific weight of "standard" air, 1.2255 kg/m^3 or 0.07651 lb./cu. ft.

3. AERODYNAMIC SYMBOLS

S, Area

S_w, Area of wing

G, Gap

b, Span

c, Chord

$\frac{b^2}{S}$, Aspect ratio

V, True air speed

q, Dynamic pressure$=\frac{1}{2}\rho V^2$

L, Lift, absolute coefficient $C_L=\frac{L}{qS}$

D, Drag, absolute coefficient $C_D=\frac{D}{qS}$

D_0, Profile drag, absolute coefficient $C_{D_0}=\frac{D_0}{qS}$

D_i, Induced drag, absolute coefficient $C_{D_i}=\frac{D_i}{qS}$

D_p, Parasite drag, absolute coefficient $C_{D_p}=\frac{D_p}{qS}$

C, Cross-wind force, absolute coefficient $C_C=\frac{C}{qS}$

R, Resultant force

i_w, Angle of setting of wings (relative to thrust line)

i_t, Angle of stabilizer setting (relative to thrust line)

Q, Resultant moment

Ω, Resultant angular velocity

$\rho\frac{Vl}{\mu}$, Reynolds Number, where l is a linear dimension (e.g., for a model airfoil 3 in. chord, 100 m.p.h. normal pressure at 15° C., the corresponding number is 234,000; or for a model of 10 cm chord, 40 m.p.s., the corresponding number is 274,000)

C_p, Center-of-pressure coefficient (ratio of distance of c.p. from leading edge to chord length)

α, Angle of attack

ϵ, Angle of downwash

α_0, Angle of attack, infinite aspect ratio

α_i, Angle of attack, induced

α_a, Angle of attack, absolute (measured from zero-lift position)

γ, Flight-path angle

REPORT No. 592

FULL-SCALE TESTS OF N. A. C. A. COWLINGS

By THEODORE THEODORSEN, M. J. BREVOORT
and GEORGE W. STICKLE

Langley Memorial Aeronautical Laboratory

141671—37——1

NATIONAL ADVISORY COMMITTEE FOR AERONAUTICS

HEADQUARTERS, NAVY BUILDING, WASHINGTON, D. C.

LABORATORIES, LANGLEY FIELD, VA.

Created by act of Congress approved March 3, 1915, for the supervision and direction of the scientific study of the problems of flight (U. S. Code, Title 50, Sec. 151). Its membership was increased to 15 by act approved March 2, 1929. The members are appointed by the President, and serve as such without compensation.

GEORGE W. LEWIS, *Director of Aeronautical Research*

JOHN F. VICTORY, *Secretary*

HENRY J. E. REID, *Engineer in Charge, Langley Memorial Aeronautical Laboratory, Langley Field, Va.*

JOHN J. IDE, *Technical Assistant in Europe, Paris, France*

TECHNICAL COMMITTEES

AERODYNAMICS
POWER PLANTS FOR AIRCRAFT
AIRCRAFT MATERIALS
AIRCRAFT STRUCTURES
AIRCRAFT ACCIDENTS
INVENTIONS AND DESIGNS

Coordination of Research Needs of Military and Civil Aviation

Preparation of Research Programs

Allocation of Problems

Prevention of Duplication

Consideration of Inventions

LANGLEY MEMORIAL AERONAUTICAL LABORATORY

LANGLEY FIELD, VA.

Unified conduct, for all agencies, of scientific research on the fundamental problems of flight.

OFFICE OF AERONAUTICAL INTELLIGENCE

WASHINGTON, D. C.

Collection, classification, compilation, and dissemination of scientific and technical information on aeronautics.

REPORT No. 592

FULL-SCALE TESTS OF N. A. C. A. COWLINGS

By THEODORE THEODORSEN, M. J. BREVOORT, and GEORGE W. STICKLE

SUMMARY

A comprehensive investigation has been carried on with full-scale models in the N. A. C. A. 20-foot wind tunnel, the general purpose of which is to furnish information in regard to the physical functioning of the composite propeller-nacelle unit under all conditions of take-off, taxying, and normal flight. This report deals exclusively with the cowling characteristics under conditions of normal flight and includes the results of tests of numerous combinations of more than a dozen nose cowlings, about a dozen skirts, two propellers, two sizes of nacelle, as well as various types of spinners and other devices.

The optimum shape of a low-drag cowling has been determined. The shape of the leading edge and the contours of the exit passage are the cause of large losses when improperly designed. The importance of providing means for regulating the quantity of cooling air to the minimum that will prevent excessive losses at high speeds has been demonstrated. The N. A. C. A. cowlings show a remarkably high efficiency when considered as a pump for the cooling air. The superiority of a baffled over an unbaffled engine has been verified and it has, furthermore, been shown that tightly fitting baffles are superior to the deflector type.

INTRODUCTION

The general purpose of a cowling has been known for some time. The original tests of N. A. C. A. cowlings are given in reference 1 and later studies in references 2, 3, and 4. The actual design of the engine cowling has, however, been based on a very inadequate scientific knowledge of its functions, owing largely to a lack of conclusive experimental data. The two basic functions of the engine cowlings are: (1) To provide an engine enclosure having minimum air resistance and (2) to act as a pump for the air that is to cool the engine or the radiator.

The cowling is usually designed to fit tightly about the engine unit with a rearward taper gradually faired into a wing or with a slightly expanding section that forms the front portion of a fuselage. The design of the portion ahead of the engine has been quite haphazard and often aerodynamically poor. As the cowling has a leading edge quite similar to that of an airfoil, it must be expected to react aerodynamically in much the same manner. The leading edge being fairly thin, the cowling must be sensitive to the "angle of attack" of the local air flow at the leading edge. This question has, in fact, been considered as a direct consequence of the findings of reference 5, in which an "ideal angle of attack" is defined.

No information has been available until quite recently on the function of the cowling as an air pump.

Since the summer of 1935 the N. A. C. A. has been conducting a very extensive investigation of propellers, nacelles, and cowlings with numerous special devices including a dozen different cowlings with a variety of skirts. Attention is being paid to the mutual interference of the parts and to their effect on engine cooling. This first report comprises the results of the tests of cowlings, nacelles, and spinners under normal-flight conditions.

ANALYSIS OF THE PROBLEM

As previously stated, the two primary functions of the cowling are: (1) To provide an engine enclosure of minimum drag and (2) to pump the cooling air through the engine or the radiator. These functions are distinct because the definite amount of work required to be done on the cooling air is distinctly different from the ordinary aerodynamic drag of the cowling itself. In order to cool the engine, a certain quantity of air Q has to be forced through the engine per second at a certain pressure difference Δp. A related increment is observed in the drag $D-D_0$ at an air speed V. The work done per second is thus $Q\Delta p$ and the work expended exclusively for cooling is $(D-D_0)\ V$, which gives an efficiency of pumping

$$\eta_p=\frac{Q\Delta p}{(D-D_0)V}$$

The quantity D_0, which is given considerable significance, is defined as the drag of a closed cowling with major dimensions similar to those of the actual cowling as indicated by the sketch in figure 1. (See also the actual design in fig. 4, nose 19, skirt 5.)

Writing the total drag of the cowling-nacelle unit

$$D=\frac{Q\Delta p}{\eta_p V}+D_0$$

the problem is stated. It is, of course, evident that η_p should be as large and D_0 should be as small as possible.

Thus far the presence of a propeller has been ignored. On first consideration one might be led to believe the propeller to be nonessential in the sense that all conclusions drawn from a test without a propeller might readily be applied. That such a procedure is not permissible will be evident from the results. The main interaction may, however, be fairly well isolated and described. In order to determine the pump efficiency with a propeller, the net efficiency of the propeller-nacelle unit will first be defined as

$$\eta_n=\frac{RV}{P}$$

where R is the thrust of the unit and P the power supplied to the propeller shaft. The value η_n thus includes the useful expenditure to cooling.

As the propeller is a secondary consideration, it will be treated very simply as a disk capable of producing the desired pressure difference or forward thrust. The velocity increase and the contraction of the slipstream

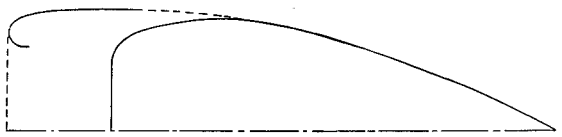

FIGURE 1.—Basic cowling shape for determining minimum drag.

are found to be proportional to the unit disk loading, defined as

$$P_c=\frac{P}{qSV}$$

where q is the dynamic pressure $\frac{1}{2}\rho V^2$ and S is the disk area $\frac{\pi}{4}D^2$.[1]

Any combinations of P, S, and q (or of V) that give fixed values of P_c are therefore essentially similar in geometrical appearance of the flow field. In the study of the effect of the propeller on the cowling, the parameter P_c will frequently be employed, or rather the more convenient expression

$$\frac{1}{\sqrt[3]{P_c}}=V\sqrt[3]{\frac{\frac{\pi}{4}D^2\frac{1}{2}\rho}{P}}=V\sqrt[3]{\frac{\rho S}{2P}}$$

It may be noted that large values of $\frac{1}{\sqrt[3]{P_c}}$ correspond to small contractions and vice versa.

An expression for the pumping efficiency of the cowling for the power tests is obtained by recognizing the fact that part of the apparent loss in aerodynamic efficiency reappears as useful work in cooling the engine. The net efficiency pertaining to a certain installation has been given as η_n, which is experimentally determined for several values of P_c. The mechanical cost of the cooling is determined by employing the closed cowling in figure 1 to obtain a series of points on the net-efficiency curve for this limiting case of no cooling or pumping losses. This particular net efficiency is denoted as η_0. A comparison of these net efficiencies at a value of P_c representing a desired standard condition gives the pump efficiency at P_c as

$$\eta_p=\frac{Q\Delta p}{(\eta_0-\eta_n)P}$$

Consider for a moment the product $Q\Delta p$. The engine or the radiator permits a rate of flow Q at a pressure difference Δp. For a given engine the pressure drop across the baffles is obviously very nearly proportional to the square of the volume and to the density ρ. A nondimensional quantity can easily be obtained. Let A be the cross-sectional area of the portion of the main air stream in front of the engine, which actually enters the engine as cooling air. (See fig. 21(d).) For a given engine or radiator this volume AV is proportional to $\sqrt{\frac{\Delta p}{q}}$; that is, the area is proportional to $\sqrt{\frac{\Delta p}{q}}$. The constant of proportionality may be defined as

$$k=\frac{A}{\sqrt{\frac{\Delta p}{q}}}$$

where k is seen to represent an area. In order to obtain a nondimensional expression, k may be expressed in terms of some representative area, such as the cross-sectional area of the nacelle F. Thus

$$K=\frac{k}{F}=\frac{\frac{A}{F}}{\sqrt{\frac{\Delta p}{q}}} \tag{1}$$

The term K, which shall be termed "the conductivity of the engine," is now a pure number. It is easy to visualize when Δp is equal to q: when the available head is used across the resistance. In this case $K=\frac{A}{F}$ and the conductivity K may be defined as the fraction of the total air column with a cross section equal to that of the nacelle that enters the inside of the cowling when the pressure drop across the resistance is equal to the velocity head q.

The term "conductivity" has been used from time to time in various forms by other authors. It is adopted because of a certain analogy to electrical terminology, as will be discussed later.

The value of $\Delta p/q$ is nearly unity in baffled engines and K normally lies between 0.05 and 0.1. Most of the reported tests were conducted with tightly fitted baffles, in which case the value of K is 0.0424. This value of K is referred to as "standard baffling." Subsequent tests were run with loosely fitting baffles in which K was 0.0909. A final series of tests was made with the baffles removed and K, approximately 0.5.

[1] It is noted that the power supplied to the air stream as thrust is somewhat less than P and that the effective disk area is reduced by the Goldstein effect. (See reference 6.)

The great convenience of having the engine-flow resistance given by a single number can be realized. If the defined quantity K is used to obtain an expression for the quantity of the cooling air

$$Q=K\sqrt{\frac{\Delta p}{q}}\,FV \tag{2}$$

a form is obtained that is particularly convenient inasmuch as a single calibration suffices to determine K for each engine baffle or radiator. The method of calibration will be described later.

Introducing K in the efficiency formulas, there is obtained for the nacelle tests with $D=C_D\,Fq$

$$\eta_p=\frac{K\left(\frac{\Delta p}{q}\right)^{3/2}}{C_D-C_{D_0}} \tag{3}$$

as the final formula for the pump efficiency. Similarly for the propeller tests

$$\eta_p=\frac{K\left(\frac{\Delta p}{q}\right)^{3/2}FVq}{(\eta_0-\eta_n)P}=\frac{K\left(\frac{\Delta p}{q}\right)^{3/2}}{\eta_0-\eta_n}\,\frac{F}{P_cS}$$

or

$$\eta_p=C\,\frac{\left(\frac{\Delta p}{q}\right)^{3/2}}{\eta_0-\eta_n} \tag{4}$$

where $C=\frac{KF}{SP_c}$. This formula is convenient as K is a constant, as are the disk area S and the nacelle cross-sectional area F. It will later be shown that the value of $\frac{1}{\sqrt[3]{P_c}}=1.8$ has been chosen as a standard of reference.

The influence of the exit area on the flow through the cowling is best explained by reference to figure 2.

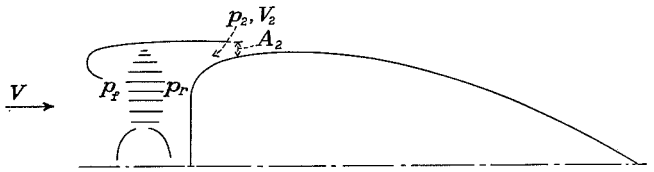

FIGURE 2.—Pressures and velocities for defining conductivity.

Observe that p_2 and V_2 are the pressure and velocity, respectively, in the exit. The static pressure p_2 is practically identical with the static pressure of the outside flow at the slot because the flow line dividing the external and internal fields is nearly straight. The expression for the total available drop is thus

$$\Delta P=\Delta p+\Delta p_2$$

where ΔP is the total head on the front minus the static pressure at the exit. The static pressure at the exit, as will be seen from a number of pressure plots, is usually slightly negative and may in some cases reach a value of $-0.3\,q$. The frontal pressure is fairly close to q on all normal cowlings. The pressure ΔP thus ranges from approximately 1 q to 1.3 q. The right-hand terms of the foregoing equation are the pressure drop across the engine and the pressure to produce the velocity head in the exit. The preceding equation written in nondimensional form is

$$\frac{\Delta P}{q}=\frac{\Delta p}{q}+\frac{\Delta p_2}{q}$$

For the pressure drop across the engine there has already been obtained the relation

$$Q=K\sqrt{\frac{\Delta p}{q}}\,FV$$

or

$$\frac{\Delta p}{q}=\left(\frac{Q}{KFV}\right)^2$$

For the pressure that produces the velocity head in the exit, there is simply

$$\Delta p_2=\frac{1}{2}\rho V_2^2$$

as the internal-friction loss in the passage is considered negligible. Inasmuch as $V_2=\frac{Q}{A_2}$ and $q=\frac{1}{2}\rho V^2$, there may be written

$$\frac{\Delta p_2}{q}=\left(\frac{Q}{A_2V}\right)^2$$

The area of the exit of the slot A_2 may be written in coefficient form as a fraction of the maximum cross-sectional area F, as K_2F. Then

$$\frac{\Delta p_2}{q}=\left(\frac{Q}{K_2FV}\right)^2$$

and for the total pressure drop the final relation [2]

$$\frac{\Delta P}{q}=\left(\frac{Q}{KFV}\right)^2+\left(\frac{Q}{K_2FV}\right)^2=\left(\frac{Q}{FV}\right)^2\left[\frac{1}{K^2}+\frac{1}{K_2^2}\right] \tag{5}$$

representing the case of two resistances in series. The pressure drop $\frac{\Delta P}{q}$ corresponds to the voltage V, the square of the rate of flow $\left(\frac{Q}{FV}\right)^2$ to the current J, and the conductivities K to $\sqrt{C}$.

A few remarks on the foregoing equation of flow regulation may be in order. Restating, the left-hand side is independent of air speed and is equal to slightly more than unity. Even with the use of cowling flaps the increase is only from about 1.1 to 1.3. The associated increase in Q is thus of the order of 10 percent and the increase in cooling is very slight. Indeed, if K is of the usual small value of baffled engines, not much is gained by increasing also the exit conductivity K_2. Representative values of K and K_2 as used in the most efficient and satisfactory installations tested are 0.05 and 0.15, respectively. The pressures across the resistances are therefore $\frac{1}{(0.05)^2}$ and $\frac{1}{(0.15)^2}$, or in the ratio [3] of 9 to 1. Any possible increase in K_2 results in only a negligible increase of Q.

[2] Note the electrical analogy, $V=J\left(\frac{1}{C}+\frac{1}{C_1}\right)$.

[3] For constant cooling, this ratio decreases as the air speed increases.

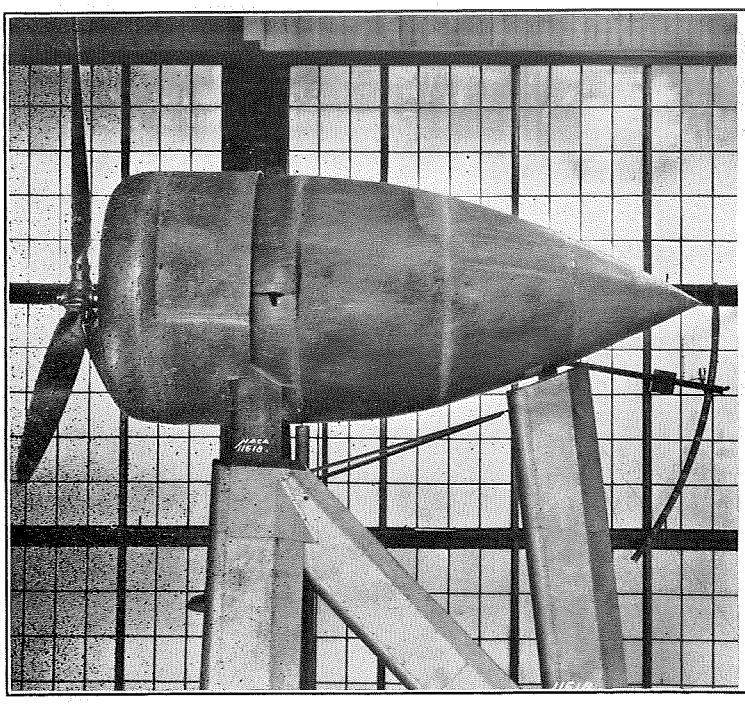

(a) Nacelle 2, nose 7, skirt 6, propeller B, inner cowling 6 (7—6—B—6—0).

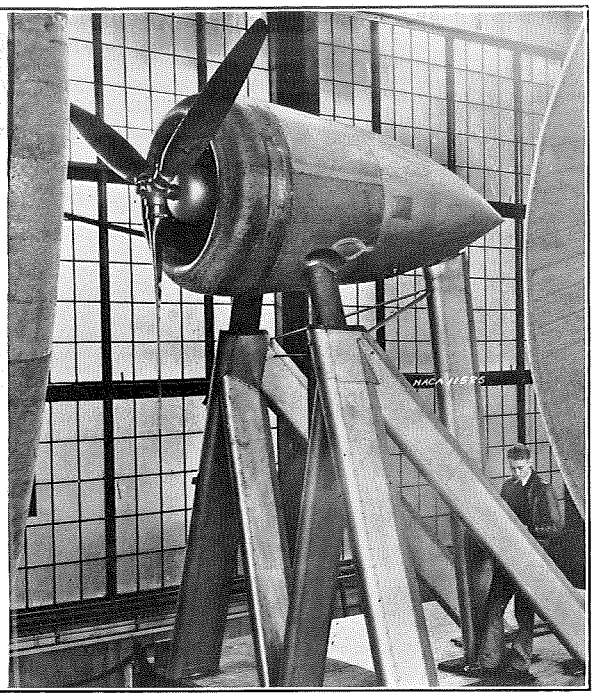

(b) Nacelle 1, nose 7, skirt 5, propeller B, inner cowling 3 (7—5—B—3—0).

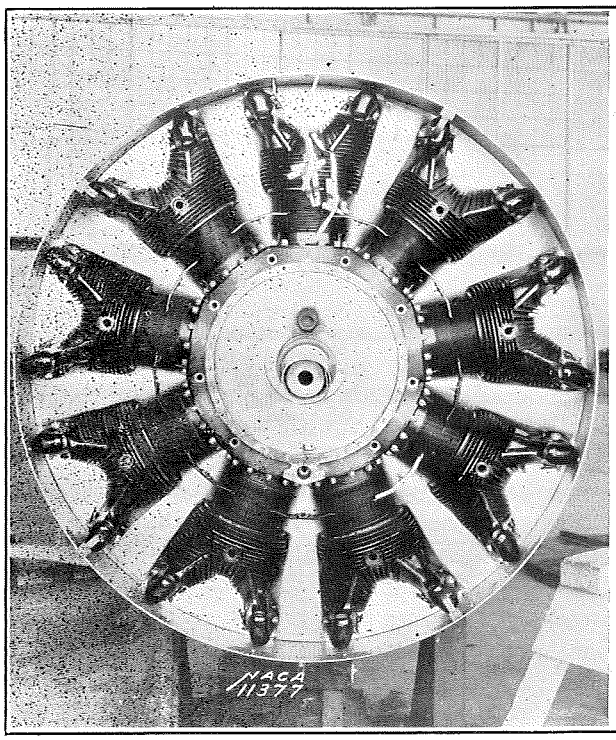

(c) Front view of engine cylinders with baffles and center section of the cowling.

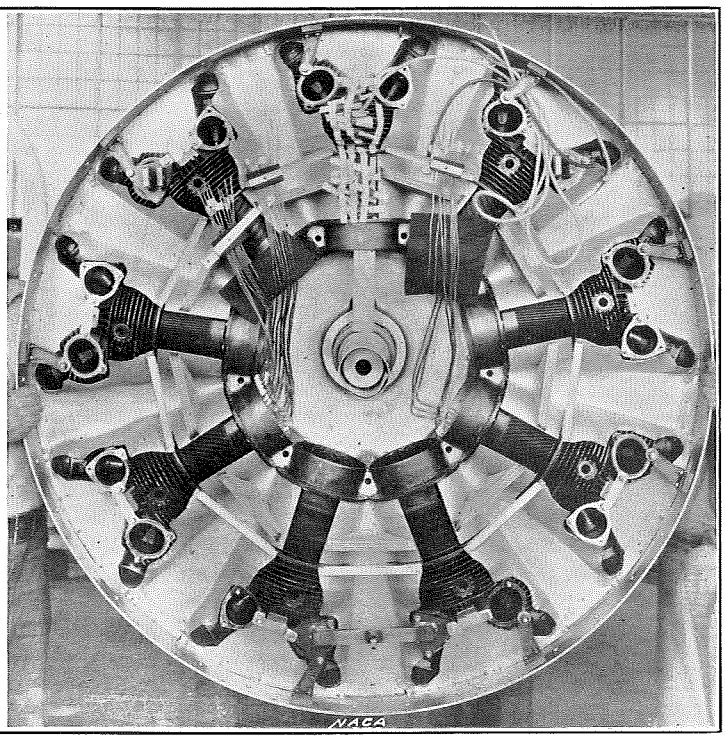

(d) Rear view of engine cylinders with baffles and center section of the cowling.

FIGURE 3.—The test set-up.

The conductivity K completely represents the engine as regards the aerodynamic tests of the nacelle-propeller unit.

The choice of the value of 1.8 is made strictly for the convenience of comparison. Each individual propeller was tested over a complete range of angles of attack. A plot of the net efficiency against $\frac{1}{\sqrt[3]{P_c}}$ shows that the range of $\frac{1}{\sqrt[3]{P_c}}$ extends from 0 to about 3, the net efficiency becoming zero at the latter point. This particular shape of the efficiency curve is, of course, a function of the present test set-up, which consists solely of an engine-nacelle unit. It is obvious that the presence of a wing section or of an entire airplane would change the shape of the entire curve. It is fairly safe to assume, however, that the differences in propellers, cowlings, spinners, etc., would manifest themselves in the same relative manner.

The condition $\frac{1}{\sqrt[3]{P_c}}=1.8$ might be more easily kept in mind as a fixed slipstream contraction; it is used to permit a comparison of the effect of the propeller on the cowling-nacelle unit under equal or similar conditions of flow.[4]

APPARATUS

The cowling investigation was conducted in the N. A. C. A. 20-foot wind tunnel, which with its standard equipment is described in reference 7. The full-scale cowling model was attached to the standard balance frame by the supports shown in figures 3 (a) and 3 (b). The supports were shielded from the air stream in the regular manner to minimize tare drag. The cowlings were built to enclose a Pratt & Whitney Wasp engine having a maximum diameter of 52 inches. The dummy engine used in the main series of tests consisted of Wasp engine cylinders mounted on the front half of the crankcase (figs. 3 (c) and 3 (d)). The engine was pivoted on an axis at the top (fig. 4) and the force was taken by a bell crank connected to a scale at the bottom. This arrangement permitted the direct determination of the axial force on the engine and the ring-cowling assembly.

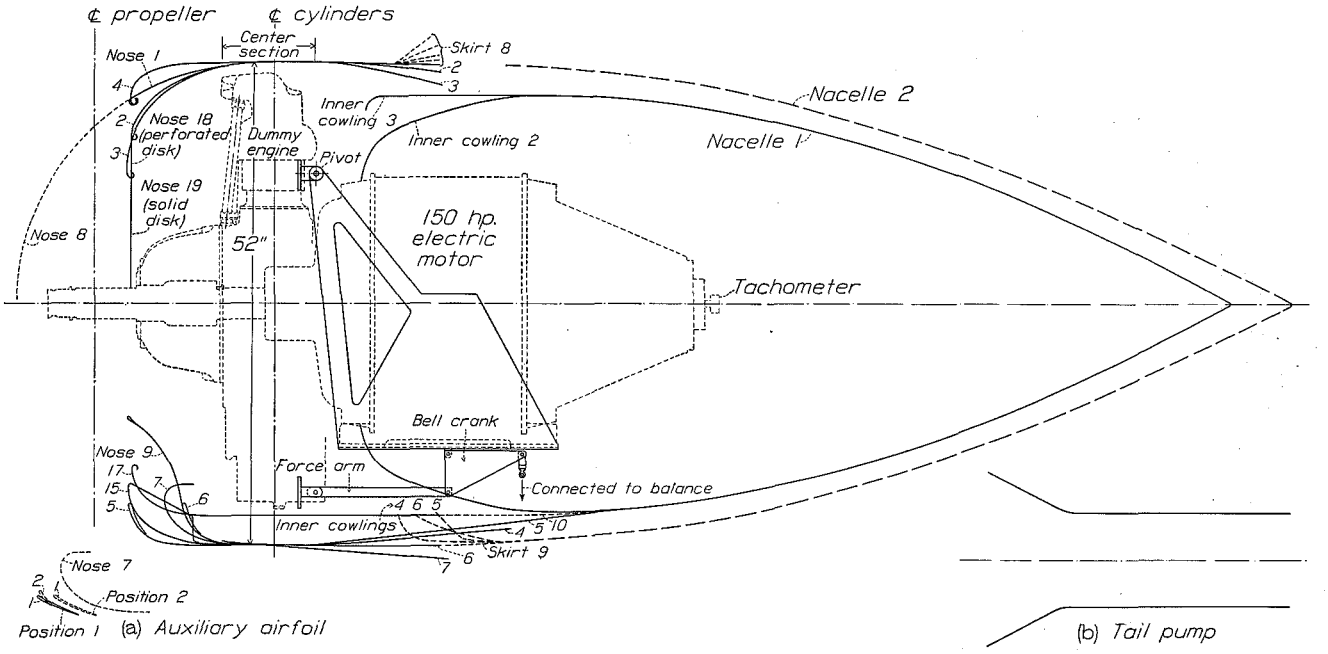

FIGURE 4.—Test model lay-out with cowling shapes.

A 150-horsepower, 3-phase, wound-rotor induction motor was mounted in the nacelle behind the dummy engine (fig. 4). This motor was calibrated in a special brake test over the entire range of speed and torque. The propeller was mounted in proper relation to the engine by an extension shaft, which replaced the engine shaft. The speed and the power output were controlled by resistance in the rotor circuit. This arrangement permitted a flexibility and accuracy far superior to those obtainable on an engine run on its own power. Another important reason for the electric drive is its dependability. With the complex installation comprised of more than 100 pressure tubes and several dozen thermocouples all over the unit, mechanical repairs would have been cumbersome.

[4] For example, the value $1/\sqrt[3]{P_c}=1.8$ is represented by a 550-horsepower engine and a 10-foot propeller at about 180 miles per hour or by a 200-horsepower engine and an 8-foot propeller at about 150 miles per hour.

The heat transmission through the cylinders was obtained by the employment of a 2-kilowatt electric heater of fixed output mounted inside cylinder 1, which was completely sealed. The measured surface temperatures thus furnished an accurate index of the coefficient of heat transmission, not subject to the multiplicity of errors associated with tests of a gasoline engine. These temperatures will be referred to in the text and tables as "index" temperatures T_i. A short preliminary series were run on an actual engine, a Pratt & Whitney Wasp S1H1–G, baffled in the average manner and run by its own power. Conductivity and temperature distribution were measured in several cases for reference purposes.

Cowlings.—All cowlings used in this investigation are surfaces of revolution about the propeller axis. The

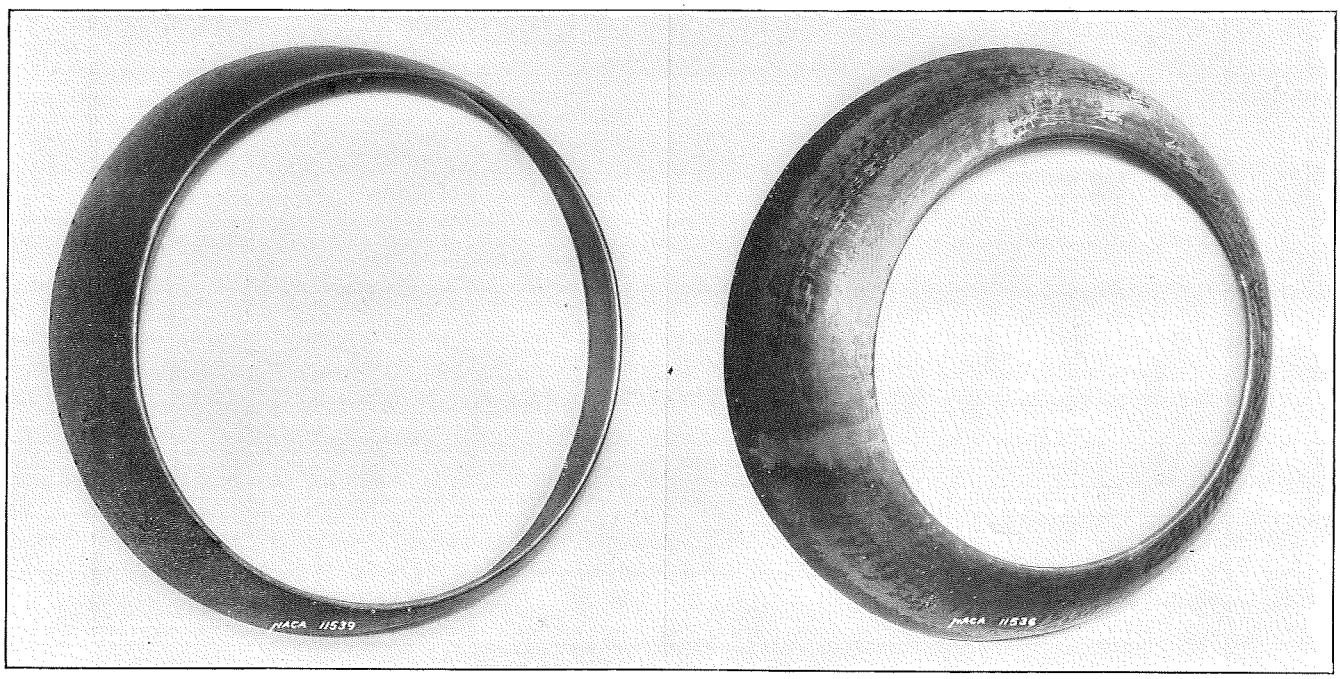

Nose 1 FIGURE 5.—Nose shapes of cowlings tested. Nose 2

various forms are represented by profile lines in figure 4. For convenience, the rear portion enclosing the electric motor will be referred to as the "nacelle." The portion forward of the exit opening will be referred to as the "cowling." The cowling may be considered to consist of three parts: (1) Nose, (2) center section, and (3) skirt. The center section of the cowling is attached permanently to the engine cylinders (figs. 3(c) and 3(d)). The same center section was used throughout all tests with the exception of the single test on the complete cowling 17. The nose and skirt sections were attached to the center section, care being taken to form a continuous smooth line. A photograph of each nose shape tested is reproduced in figure 5.

The original series comprised nose shapes 1, 2, 3, and 4, all being of the same length and general construction. Noses 1 and 4 had the same size of front opening but had very different angles of attack at the leading edge. Nose 5 differed from nose 4 by having the leading edge designed as an airfoil section. Nose 6 was identical with nose 5 except for a shortening of 6 inches in the axial length. Nose 7 was designed with a greater radius of curvature than nose 6, representing a cowling very neutral to the direction of the oncoming air flow. Nose 8, which was built on the basic form of nose 1, represents a completely closed nose used for special purposes. Nose 9 is built on nose 6 with a forward reversed curvature. Nose 15 is especially designed for housing a blower attached to the propeller shaft. Nose 17 is a design to determine the effect of reducing the main diameter of the cowling by placing bumps over the rocker boxes to house them. The basic shape is shown in figure 4 and in figure 5. Nose 18 is a combination of a perforated disk and nose 2. Nose 19 is a combination of a solid plate and nose 2.

The various shapes of skirt section tested are shown in figure 4. Skirts 5, 9, and 10 closed up the rear opening to the cowling. Skirt 8 had flaps of 5-inch chord and 6-inch span turned out in the positions shown in figure 4.

Nacelles.—Nacelles 1 and 2, 44 and 50 inches in diameter, respectively, were used in this investigation. The leading contour of the nacelle formed the inner surface for the cowling slot and is termed "inner cowling." Inner cowlings 2 and 3 were used with nacelle 1; inner cowlings 4, 5, and 6 were used with nacelle 2. These inner cowlings and the nacelles are shown in figure 4.

Baffles.—Baffles of conventional shape were used in this investigation. (See figs. 3(c) and 3(d).) They were in contact with the cylinder barrel fins from the 100° position to the 145° position (see fig. 6) for the standard-baffle condition shown in table I. In order to cover different degrees of baffling in this investigation, the baffles were moved back ½ inch for a few tests. The baffles were removed for several tests, as shown in table I.

Propellers.—Two 10-foot diameter, 3-blade Hamilton Standard adjustable propellers (fig. 7) were used for these tests. Propeller B (Hamilton Standard drawing 1C1–0) has airfoil sections close to the propeller hub. Propeller C (Navy plan form 5868–9) has the round part of the shank carrying farther out on the blade and fairing slowly into an airfoil section. Propeller B_x is the same as propeller B except that the distribution of blade-angle setting beyond the 70-percent radius has been changed. A more complete description of the propellers is given in the associated report on propellers (reference 8).

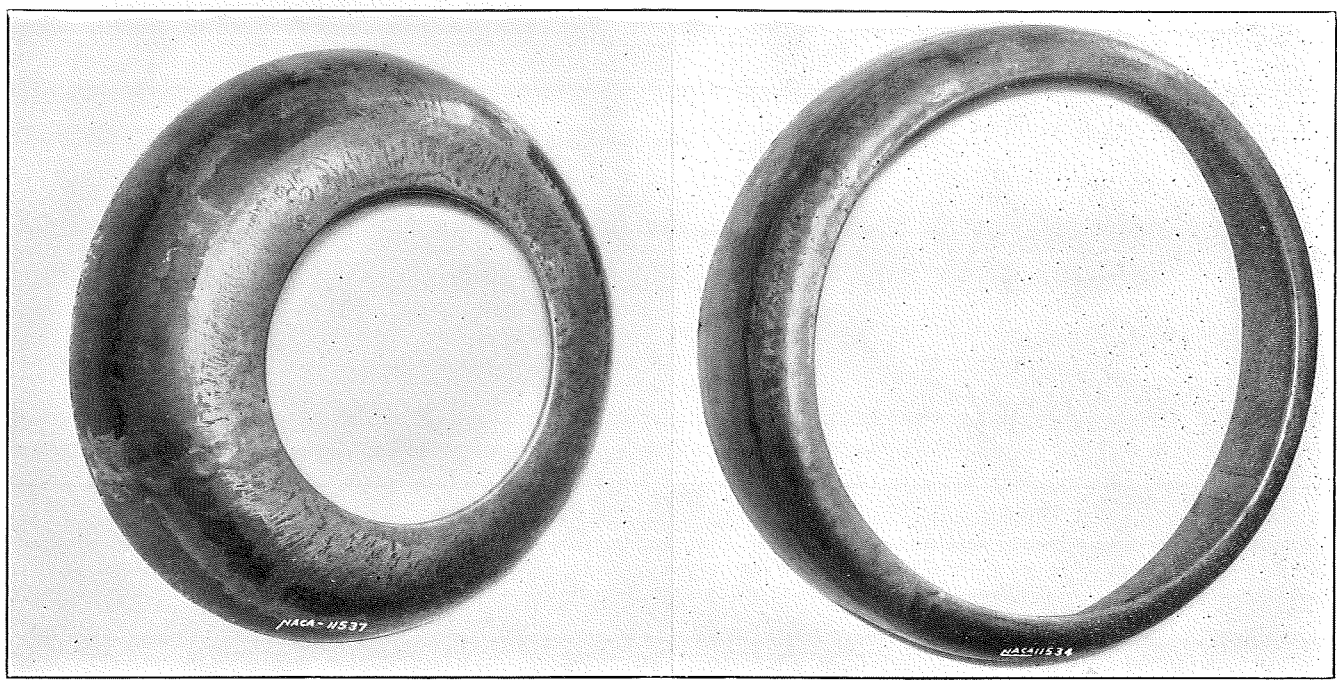

Nose 3 Nose 4

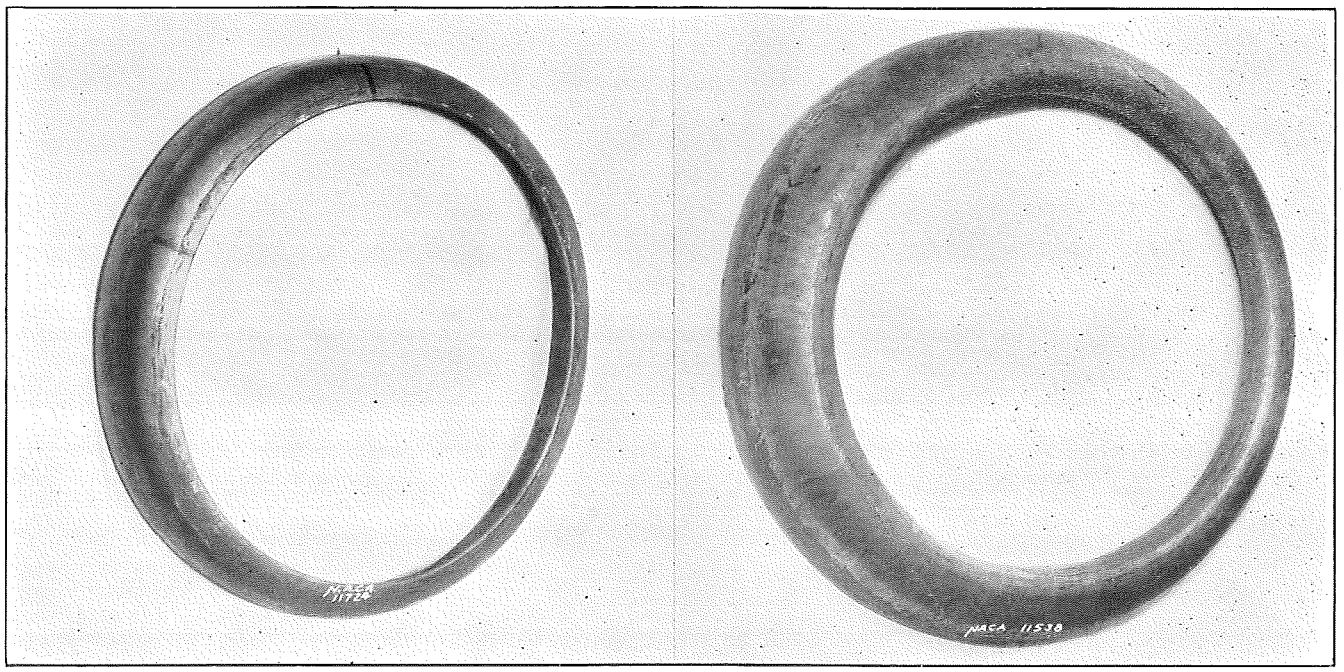

Nose 6 FIGURE 5.—Continued. Nose shapes of cowlings tested. Nose 7

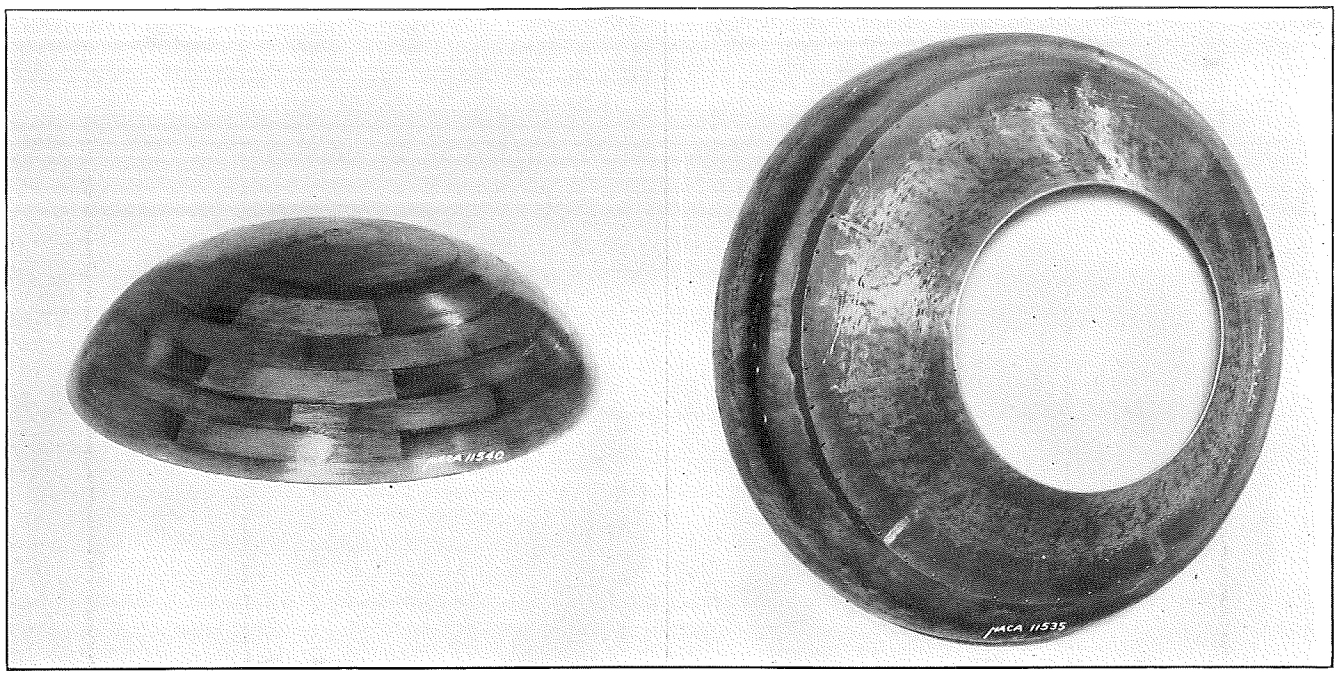

Nose 8 Nose 9

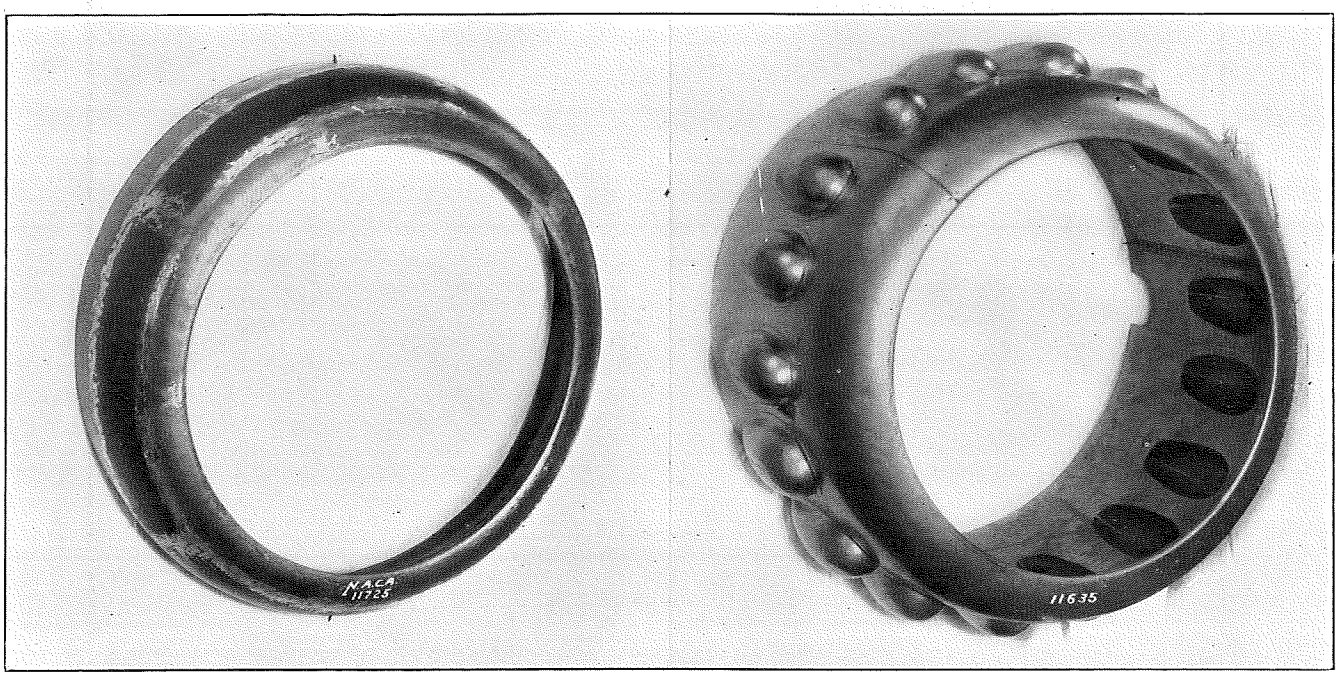

Nose 15 Nose 17

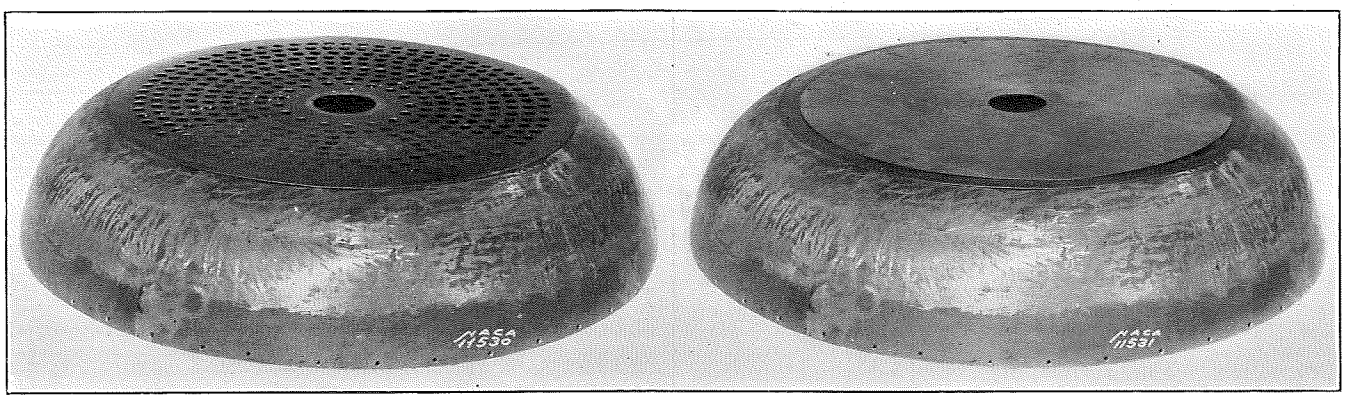

Nose 18 FIGURE 5.—Continued. Nose shapes of cowlings tested. Nose 19

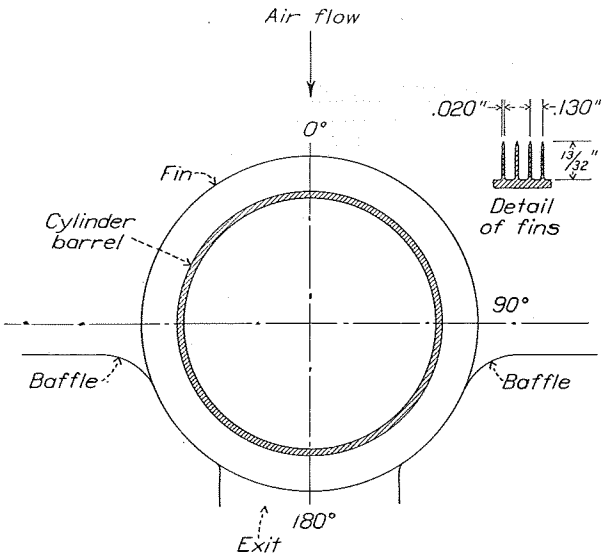

FIGURE 6.—Standard baffle arrangement.

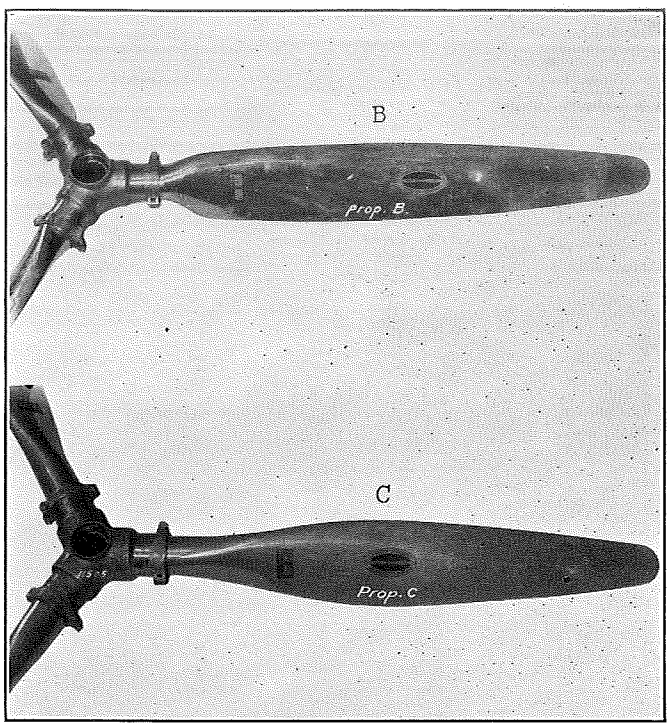

FIGURE 7.—Propellers used for the cowling tests.

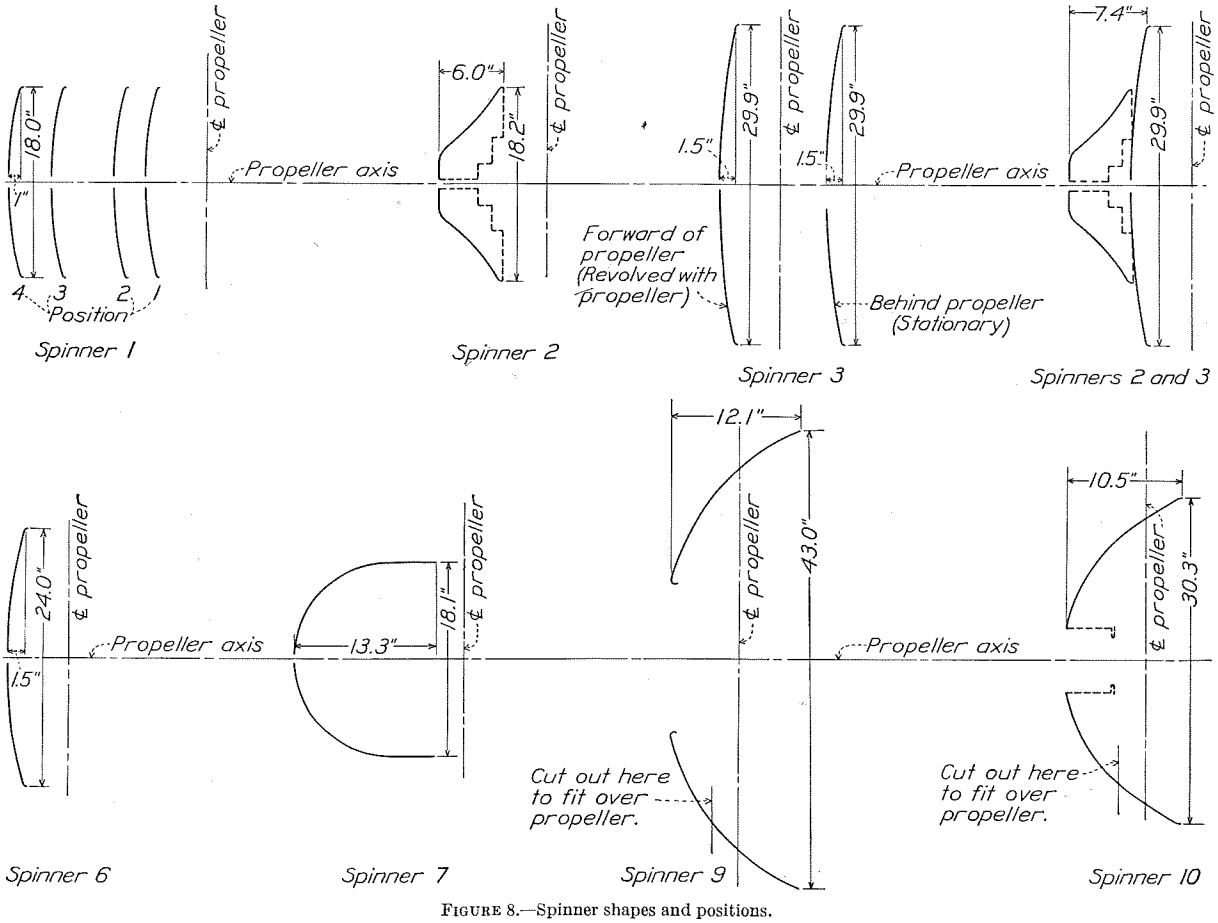

FIGURE 8.—Spinner shapes and positions.

Spinners.—Dimensioned drawings of the spinner shapes and their positions with reference to the plane of the propeller are given in figure 8. (See also fig. 9.) Spinner 9 was the only spinner that admitted air through the center.

Special devices.—Several special devices were tested in order to gain some insight into their effects on the normal arrangement.

1. Auxiliary airfoil: A circular airfoil of the section shown in figure 4(a) was used in combination with

nose 7. Auxiliary airfoil 1 was tried in two positions as shown. Auxiliary airfoil 2 had the same chord as airfoil 1, but the leading edge was turned down as shown in the drawing. It was tried only in position 1.

2. In order to investigate the possibility of discharging the cooling air through the rear of the nacelle, the special design shown in figure 4(b) was tested. air flowed around the cylinder. Four pitot tubes and four static-pressure tubes were placed across the exit of the baffles to determine the energy in the air at that place. Sixteen pitot tubes and eight static-pressure tubes were placed in the exit of the skirt to measure the air flow through the engine. Survey tubes were placed at intervals outside the cowling surface to

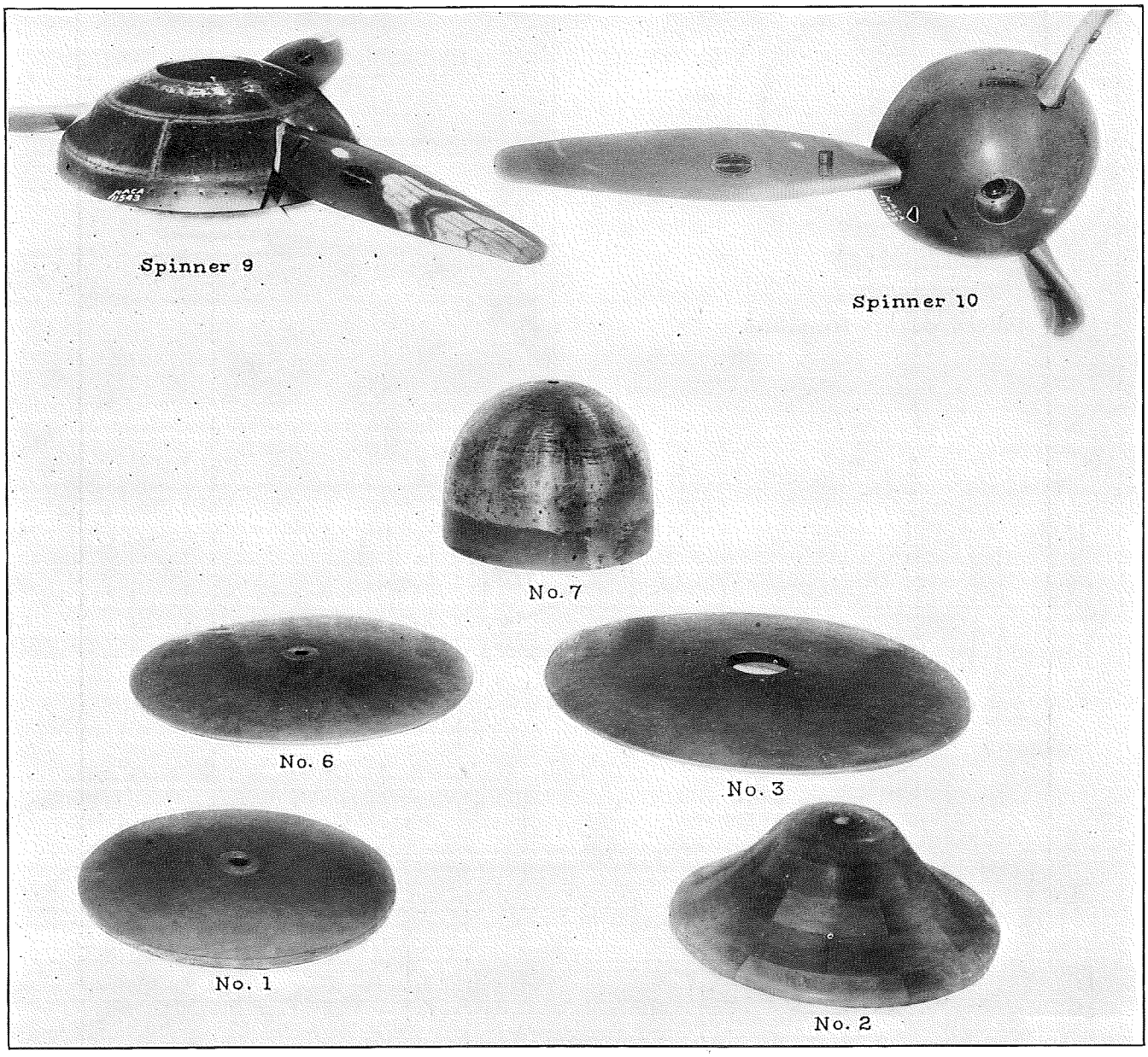

FIGURE 9.—Spinners.

Unfortunately, the resistance through the nacelle was too large to permit a sufficient range to be covered.

Pressure and temperature apparatus.—Static-pressure orifices were placed over the inner and outer surfaces of the cowling to give a sufficient number of measurements to determine the static pressure at any point on these surfaces. Twelve pitot tubes and twelve static-pressure tubes were placed between the fins on a cylinder to measure the loss in energy as the determine the flow condition with different cowling shapes. A survey was made of the air stream at six locations along the axis of the nacelle with each propeller and with no propeller.

Thermocouples were placed at positions around the cylinder corresponding to the positions of the pressure measurements. Hot-wire anemometers were used in the front and the rear of the cylinder to determine the relative cooling obtained in each place.

RESULTS

The top speed actually employed in the tunnel was approximately 100 miles per hour. The V/nD values were, however, extended to depict conditions up to 300 miles per hour at one-third the actual Reynolds Number. The present paper is confined to a report on the results of the aerodynamic properties of cowlings at normal-flight speeds. Several of the tests were also concerned with the cooling properties.

All propellers were actually tested throughout the blade-angle range of 15° to 45° (reference 8). The present report includes only propellers B and C at a blade-angle setting of 25°. The tests were actually extended over the complete range of P_c and it is entirely for convenience that the results of this paper are confined to a representation of a normal cruising condition. All conclusions in regard to the results are definitely identical with those obtainable at any other value of P_c in the cruising range. The conditions obtained in the lower end of the speed range are presented in a separate report (reference 9). The tests, in general, comprised the following measurements:

Drag, or thrust, and the power supplied.
Pressure distribution over nose, skirt, and nacelles.
Pressures in the front and rear of engine unit.
Velocities through baffles and skirt opening.
Temperatures of heated-cylinder barrel.

Table I summarizes the condensed results pertaining to the experiments on cowlings under a cruising condition and includes pertinent related information. The subdivisions relate to specific variables. The main division is on the basis of conductivity with secondary divisions for the nacelles, spinners, and other special devices.

Each unit was given a designation made up of five numbers or letters separated by dashes. These numbers refer to the parts of the unit shown in figure 4 and are, in order, nose—skirt—propeller—inner cowling—spinner. Thus 7—2—C—3—7 represents a test made on nose 7, skirt 2, propeller C, inner cowling 3, and spinner 7. A missing part is represented by the number 0. These designations are given in column 1 of table I. Column 2 is the pressure p_f in front of the engine divided by the air-stream velocity head q. Column 3 is the pressure in the rear of the engine p_r divided by q. Column 4 is the difference between columns 2 and 3, or $\Delta p/q$. Column 5 gives the values of the conventional drag coefficient $C_D=D/qF$. Column 6 gives the drag at $q=25.6$ pounds per square foot, which corresponds to a speed of 100 miles an hour at standard conditions, or the thrust at a value of $1/\sqrt[3]{P_c}$ of 1.8 at a q of 25.6 pounds per square foot. Column 7 is the net efficiency of the arrangement at the value of $1/\sqrt[3]{P_c}$ of 1.8. Column 8 presents the pump efficiency. Columns 9 and 10 give the index temperatures at the front and back, respectively, of the barrel of the electrically heated cylinder. The index temperatures are the temperature differences between the cylinder and the air stream.

FORCE MEASUREMENTS

The total drag for the test arrangement 7—2—0—3—0 for a range of q up to 28 pounds per square foot is given in figure 10. In order to have a representative picture in a particular case of the drag distribution of each part of the set-up, the pressure distribution over the whole unit is shown in figure 11(a). The values plotted are the nondimensional pressures p/q measured along the surface of the body. The recorded pressures are plotted on normals to the surface at the point where the orifice was located. Both positive and negative values are plotted on the outside of the body, the appropriate sign being indicated.

Using the same values, secondary plots (fig. 11) give the graphical integration of the axial force with the pressure plotted against the radius. The area under the plots represents the pressure drag of the body. The figures also give the individual contribution of each part, the momentum in the exit slot being included.

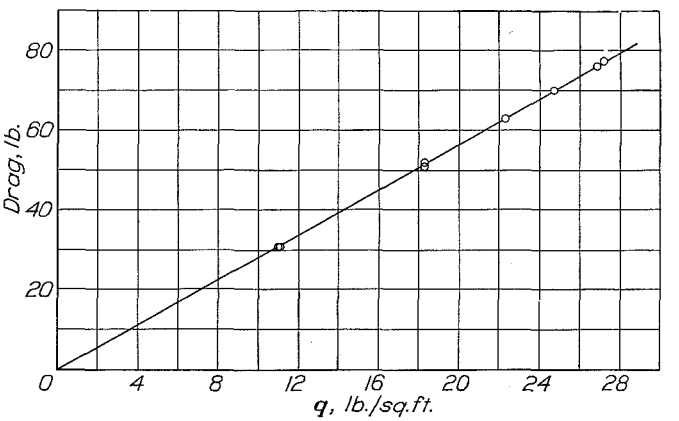

FIGURE 10.—Sample drag curve for test arrangement 7—2—0—3—0.

The actual measured drag for the unit was 72.5 pounds and the value given by the pressure plot is 57 pounds. To the latter value should be added 10 pounds, or more, estimated for the skin friction. The essential point in this comparison is not the closeness of the agreement but the picture obtained of the relative effect of the several parts of the set-up.

The same set-up was tested with propeller B operating (7—2—B—3—0). The conventional curves of propeller thrust coefficient C_T, power coefficient C_P, and propulsive efficiency η are plotted against V/nD in the usual manner (fig. 12(a)). Of more direct concern in the present paper is, however, the curve of net efficiency η_n plotted against the quantity $1/\sqrt[3]{P_c}$ (fig. 12 (b)), both quantities having been defined in the earlier analysis of the problem. As previously mentioned, the values of η_n included in table I were taken from such curves of η_n against $1/\sqrt[3]{P_c}$ for a value of $1/\sqrt[3]{P_c}$ of 1.8.

PRESSURE DISTRIBUTION

As mentioned in the introduction, the drag of an arrangement without the propeller operating is not a safe criterion of performance. This section and table I show how the pressures over the body change with propellers operating in front of the body. Under the cruising condition reported here the effect of the propeller is less marked than in the condition of climb or take-off.

From the distribution of the static pressure over the entire unit as given graphically in figure 11, an impression of the relative importance of the various parts is obtained. A study of a number of similar plots shows that the pressure drag of the rear portion, or nacelle, remains fairly constant, resulting in the important conclusion that the cause of essential differences in the drags of the several arrangements is to be found in the cowling or, more specifically, may be traced back to the nose section. Another cause of large losses may be traced back to an inefficient skirt section. An indirect effect of the nose manifests itself in a variation of the static pressure on the frontal area of the engine, this pressure being always somewhat less than the corresponding total head of the air stream. This pressure

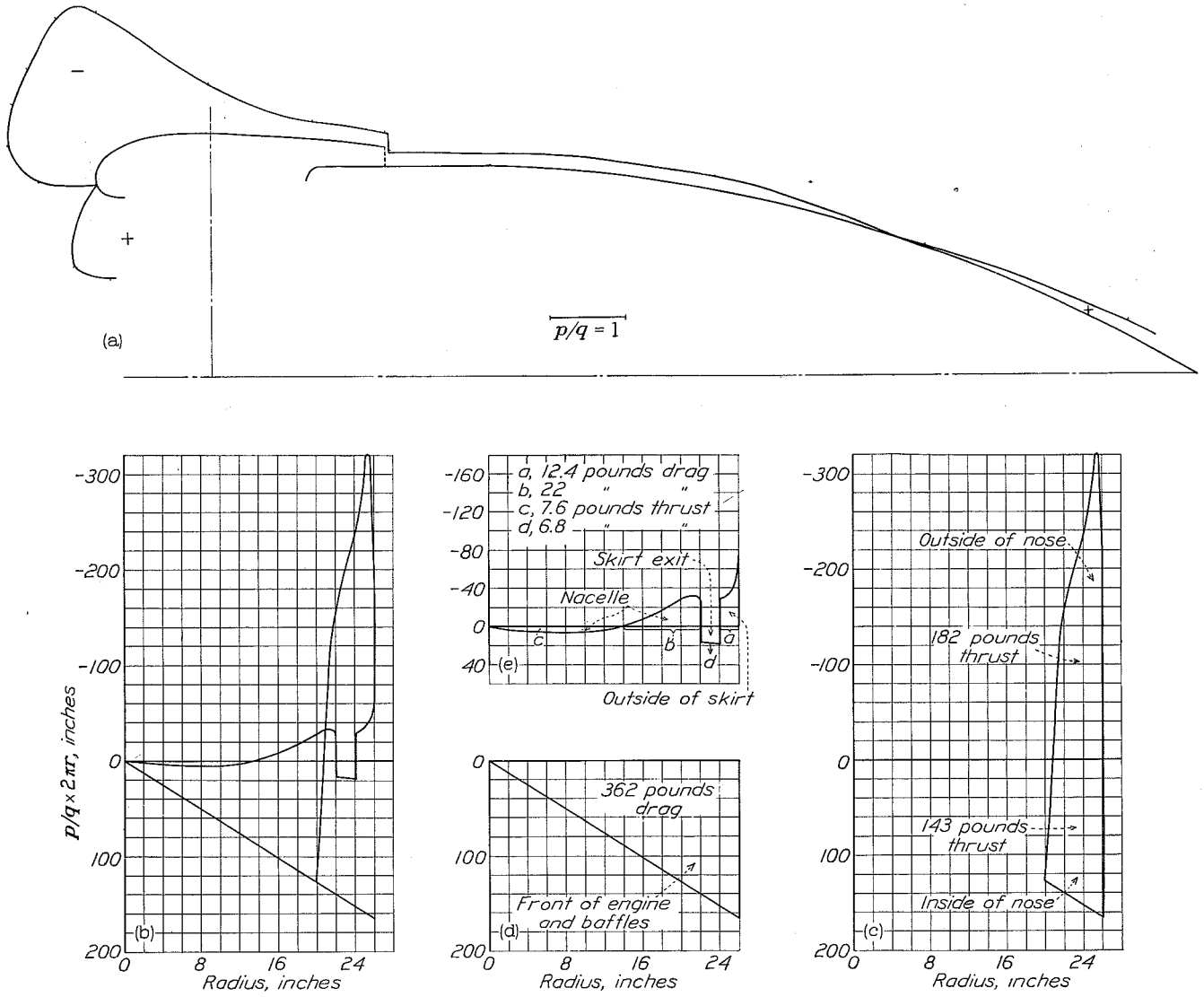

FIGURE 11.—Pressure distribution on the test arrangement 7—2—0—3—0 and the integrated drag from the pressure distribution.

From the distribution of the static pressure over the entire unit as given graphically in figure 11, an impression of the relative importance of the various parts is obtained. A study of a number of similar plots shows that the pressure drag of the rear portion, or nacelle, remains fairly constant, resulting in the important conclusion that the cause of essential differences in the drags of the several arrangements is to be found in the on the front of the engine must be measured with considerable care in order to obtain reasonable accuracy in the integrated pressure drag. An error of 0.05 q at a value of q of 25.6 pounds per square foot corresponds to an error of 19 pounds in the pressure drag.

The pressures p_f/q on the front of the engine, taken as an average of several simultaneous measurements over the area, are given in table I. The pressure distribution over a number of individual cowlings is given in figure 13. The pressure distribution over a

number of skirts tested in conjunction with nose 7 is given in figure 14. The effect of a propeller on the pressure distribution on arrangement 7—2—B—3—0 is given in figure 15 for several air speeds. The greatest value of such pressure plots lies in the possibility of qualitatively distinguishing between desirable and undesirable flow characteristics. It is possible to associate an efficient nose with a smooth distribution of the static pressure. On such a basis one would evidently select nose 2, 3, or 7.

Attention will be called to the fact that care must be taken to obtain the pressure distribution under the correct conditions. Some noses, in particular nose 1, are very critical in regard to the effect of the propeller slipstream. This effect has been referred to in the introduction as an effect of the relative direction of the local air flow with respect to the leading edge or contour of the nose. It is interesting to observe that nose 1, which is unusually inefficient at normal air speeds, approaches a reasonable efficiency at low air speeds.

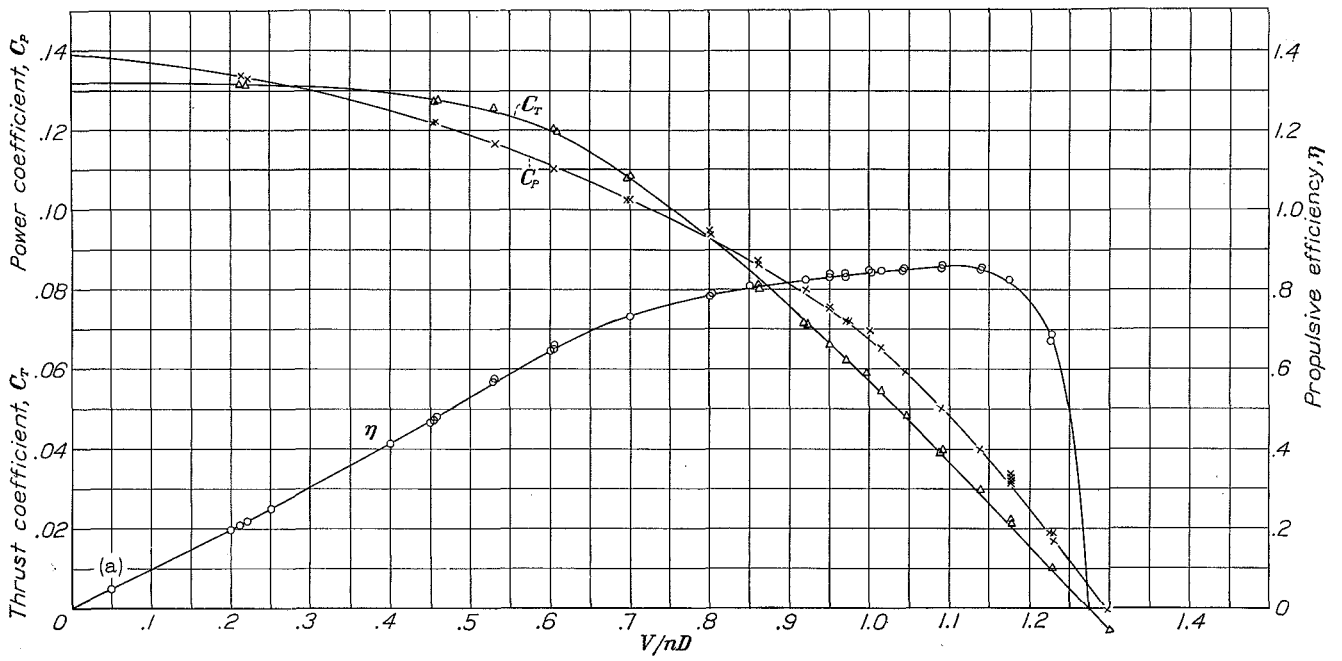

(a) Curves of C_T, C_P, and η against V/nD.

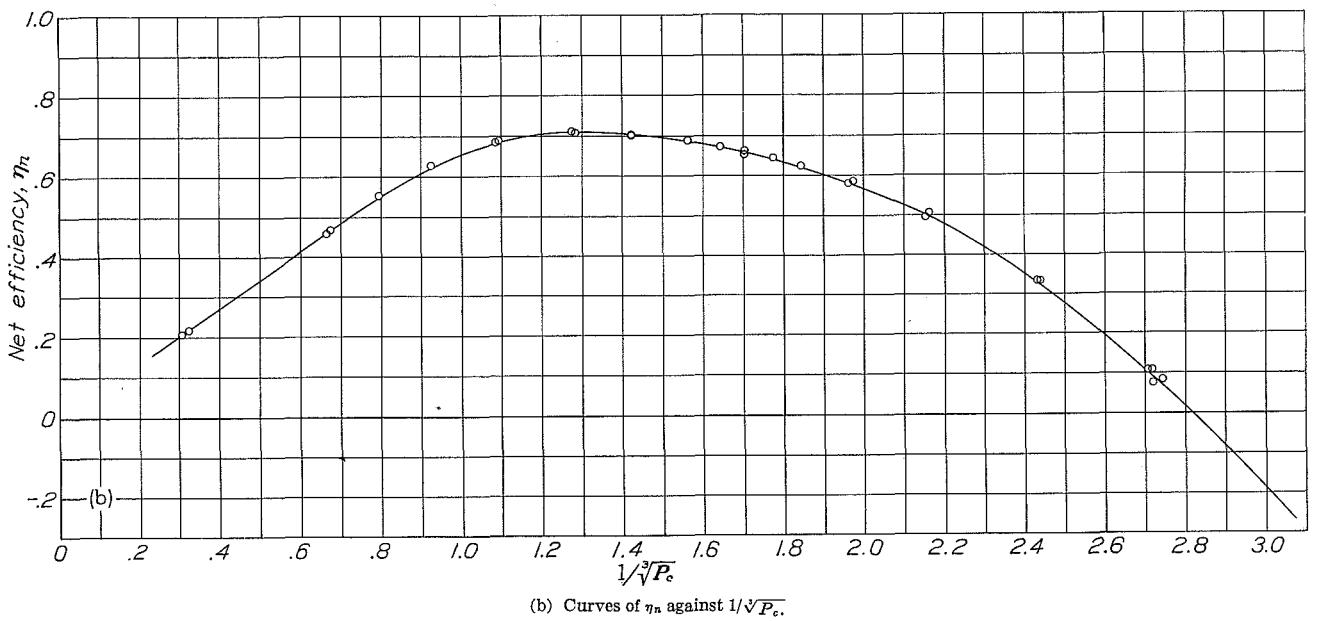

(b) Curves of η_n against $1/\sqrt[3]{P_c}$.

FIGURE 12.—Sample curves. Arrangement 7—2—B—3—0. Blade angle set 25° at 0.75R.

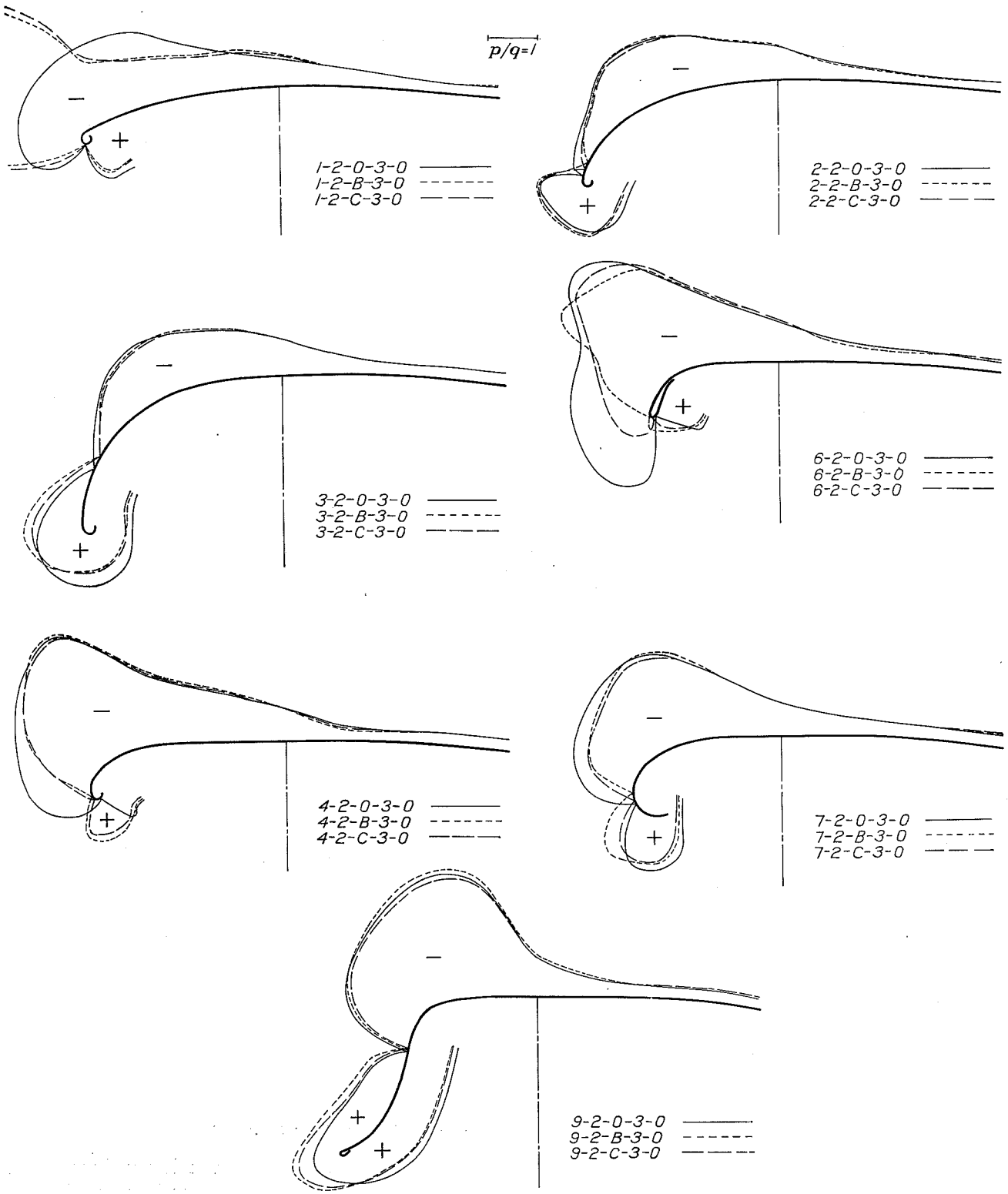

FIGURE 13.—Pressure distribution over various cowling shapes.

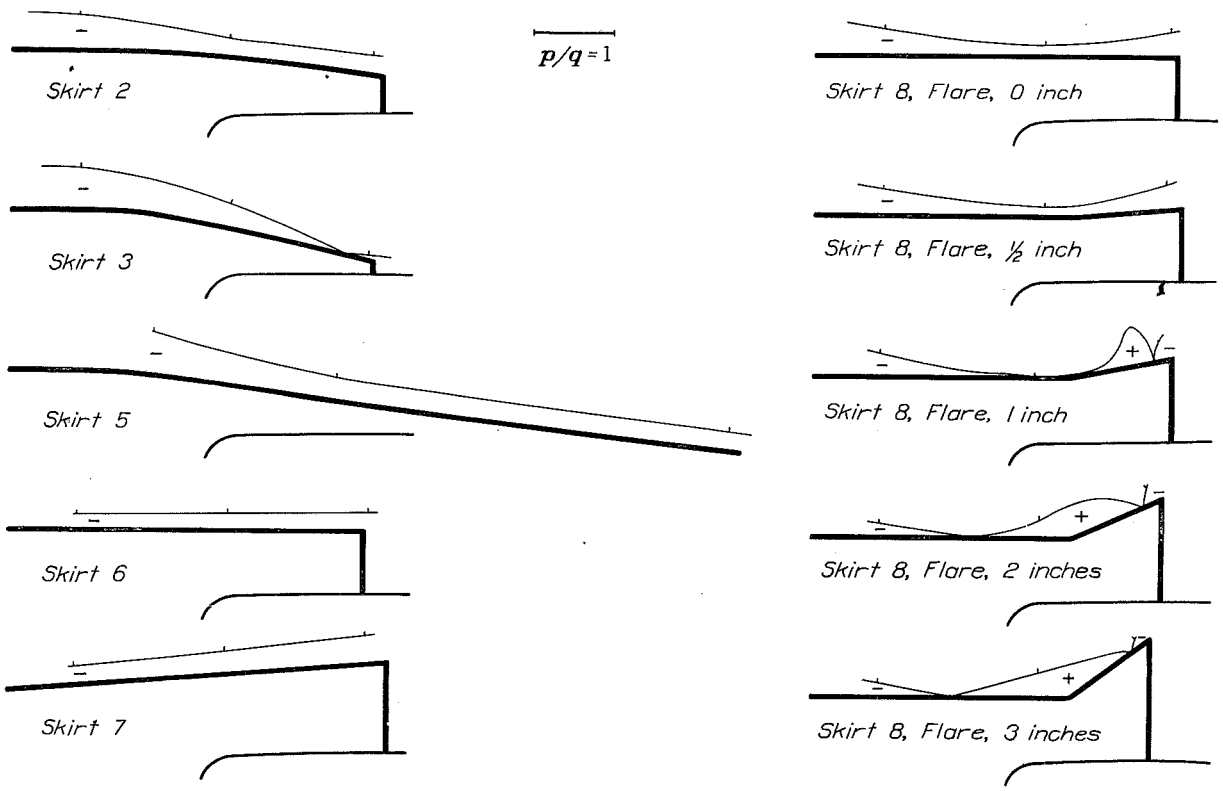

FIGURE 14.—Pressure distribution over the various skirts for test arrangement 7—X—0—3—0.

Curve	Arrangement	Propeller setting	Speed (r.p.m.)	q (lb./sq.ft.)
A	7-2-0-3-0	25° at 0.75R		25.80
B	7-2-B-3-0		648	.64
C	7-2-B-3-0		675	2.94
D	7-2-B-3-0		766	11.32
E	7-2-B-3-0		835	18.15
F	7-2-B-3-0		871	21.80

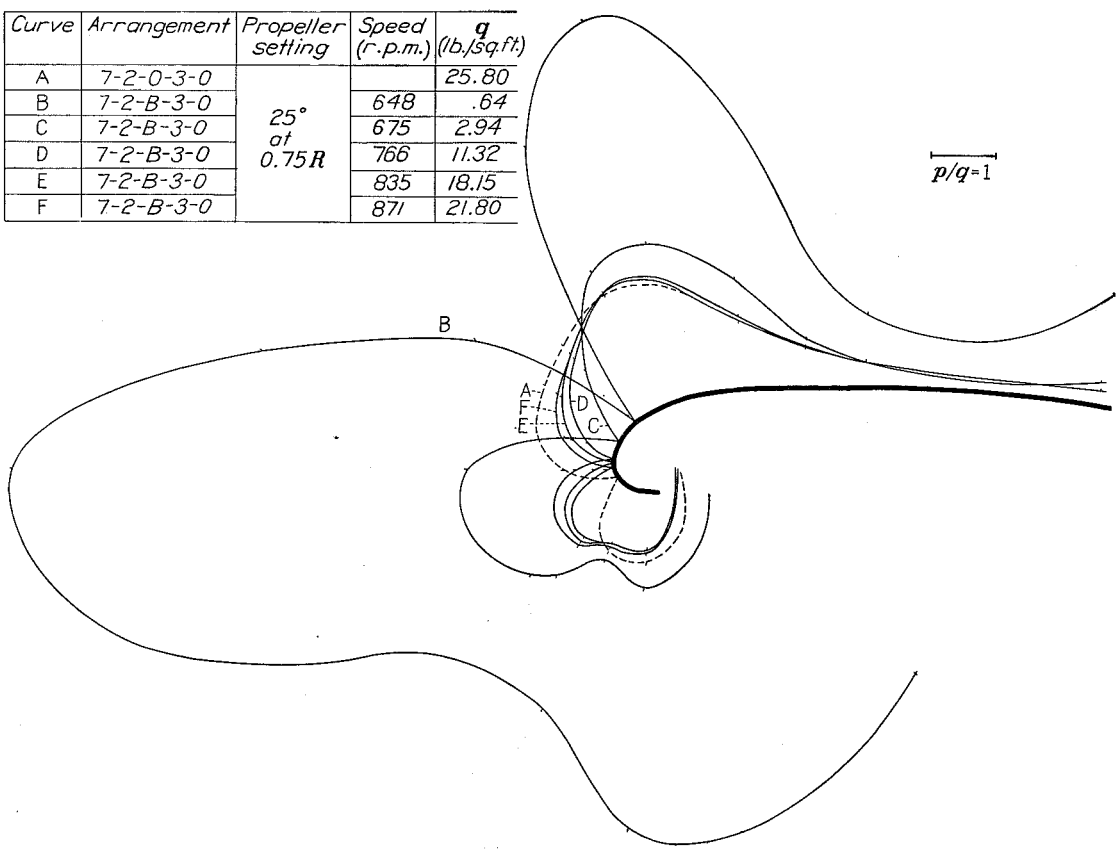

FIGURE 15.—The effect of the propeller on pressure distribution at several air speeds.

Thus with a proper consideration of the effect of Reynolds Number and the propeller slipstream, it is concluded that the pressure distribution is an excellent although somewhat indirect method for evolving an aerodynamically efficient cowling design, the procedure being to adjust the shape repeatedly until the smoothest pressure distribution is reached in whatever range may be desired. Cowling 7 was directly produced as a result of this type of procedure, this cowling being the least critical to changes in operating conditions, combined with high efficiency. The high negative pressure on the nose of the cowling is utilized in the new nose-slot cowling (reference 10) to give a higher pressure drop across the engine for cooling.

CONDUCTIVITY

The physical definition of the term "conductivity" has already been given. Two measurements are needed to determine experimentally this quantity K: the pressure drop $\Delta p/q$ across the resistance and the rate of air flow Q. The value $\Delta p/q$ is obtained directly by a system of pressure tubes placed over the front and the rear areas of the engine unit, the averages being given in table I. The rate of flow is determined by a number of permanent installations for velocity surveys across the exit opening, a total of 24 tubes, 16 impact and 8 static, being used. As previously mentioned, the conductivity is obtained by the formula

$$K=\frac{\frac{Q}{FV}}{\sqrt{\frac{\Delta p}{q}}}$$

It is to be noted that, thus defined, the quantity K is entirely a function of engine-baffle design. That this assertion is strictly true was confirmed by tests of a given baffle arrangement with a variety of different noses and skirts, all resulting substantially in the same value of K. Independence of the Reynolds Number was similarly established by tests over the entire range of air speeds. This independency of the Reynolds Number is explained by the fact that the pressure loss in the baffles consists primarily of the exit loss and is therefore nearly proportional to the square of the velocity.

Three values of conductivity are used in the present investigation:

(1) $K=0.0424$, representing the case of the baffles fitting tightly against the cylinder barrel.

(2) $K=0.0909$, representing the case of the baffles moved back ½ inch, giving a somewhat diverging channel along the back of the cylinder barrel.

(3) $K=$ about 0.5, representing the case of an unbaffled engine, the pressure drop being too small to be measured with sufficient accuracy.

The accuracy in determining the values (1) and (2) by the above-described method is within 1 percent.

These conductivities cover the useful range, as the value of the conductivity for an actual engine with commercial type of baffles of satisfactory design had been determined in the preliminary test as $K=0.06$. Deeper fins and more cylinders in parallel, as used in 2-row radials, might increase this value to as much as 0.15.

In regard to the optimum conductivity of the engine-baffle unit, it is to be observed that a minimum quantity of air is necessary to carry away a given quantity of heat. The maximum temperature difference between the air and the cylinder is of the order of 400° F. By the reduction of the quantity of cooling air, a condition is soon reached in which the effect of the reduced temperature difference more than offsets other advantages. A reasonable increase in the temperature of the cooling air on passing through the baffles is of the order of 50° to 60° F. The corresponding air quantity may be considered the minimum and the related conductivity the optimum.

The "apparent conductivity" of the skirt exit openings, defined as A_2/F, is found to be large compared with the conductivity of the engine. The pressure drop through the skirt is therefore small in comparison with the pressure across the engine, except for the narrowest skirt 3. This condition is different for the unbaffled engine. In such an engine the pressure drop is largely used to create velocity in the exit opening. It may, in consequence, be seen from table I that a value of very nearly $1q$ is available for cooling under ordinary conditions.

PUMP EFFICIENCY

It has been shown in the first part of the paper that the pump efficiency is given by formula (3)

$$\eta_p=K\left(\frac{\Delta p}{q}\right)^{3/2}\frac{1}{C_D-C_{D_0}}$$

for the case of the propeller off. Similarly, formula (4)

$$\eta_p=C\frac{\left(\frac{\Delta p}{q}\right)^{3/2}}{\eta_0-\eta}$$

is used for the power tests. The values of C_{D_0} and η_0, which quantities relate to the closed basic contour indicated in figure 1, were determined by tests of the actual shape 19—5—0—3—0 as $C_{D_0}=0.112$, or a drag of 42 pounds at 100 miles per hour, and by tests of the shape 19—5—C—3—0 as $\eta_0=74.2$ percent.

For propellers B and C the values of the constant C, representing KF/SP_c, in formula (4) at the standard value of $1/\sqrt[3]{P_c}$ of 1.8 are 0.046 and 0.099 for the conductivities K of 0.0424 and 0.0909, respectively.

The experimentally determined pump efficiencies are given in table I. These efficiencies are in strict accordance with the definition given in the introductory analysis and in complete agreement with one adopted

in reference 11. The drag obtained on the closed basic cowling shape (fig. 1) is to a certain extent arbitrary, thus permitting efficiencies in excess of unity as may be noted in a few cases. It must be realized that such a definition permits efficiencies in excess of unity, explainable by the fact that some duct arrangements improve the flow to some extent, which condition might

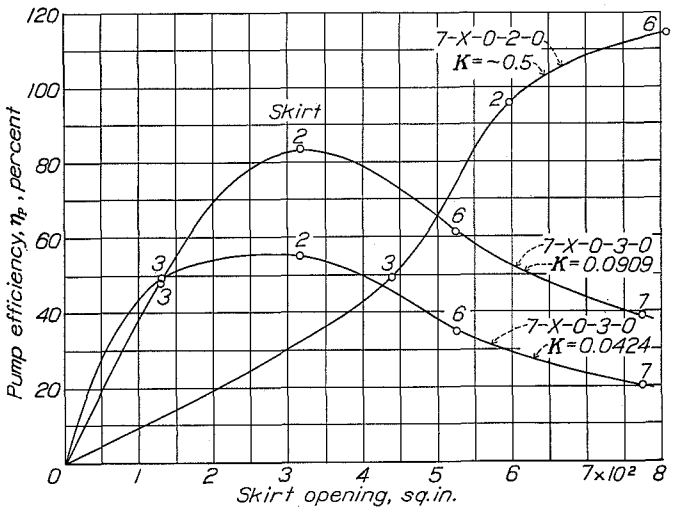

FIGURE 16.—Pump efficiency against skirt exit area for several skirts.

be expected to occur on somewhat inefficient forms, that is, forms with poor streamlining.

The table shows widely varying pump efficiencies from almost zero to more than unity (i. e., 100 percent). Some of the results are reproduced in figures 16, 17, and 18. In figure 16 the pump efficiency is plotted against the area of the exit opening; each of the three curves relate to a constant conductivity. Note that the peak efficiencies increase with the conductivity and occur at successively larger exit openings. It is to be noted that the pump efficiency depends to a considerable extent on the shape of opening and not only on its cross-sectional area. The curve for each conductivity, therefore, does not necessarily attain the optimum efficiency at each skirt size. This fact is particularly true for the small and the large skirt openings. Notice that skirt 2 yields efficiencies of from 50 to more than 80 percent for normal conductivities of baffled engines, and of 100 percent for the unbaffled engine. As might be expected, the pump efficiency is seen to increase

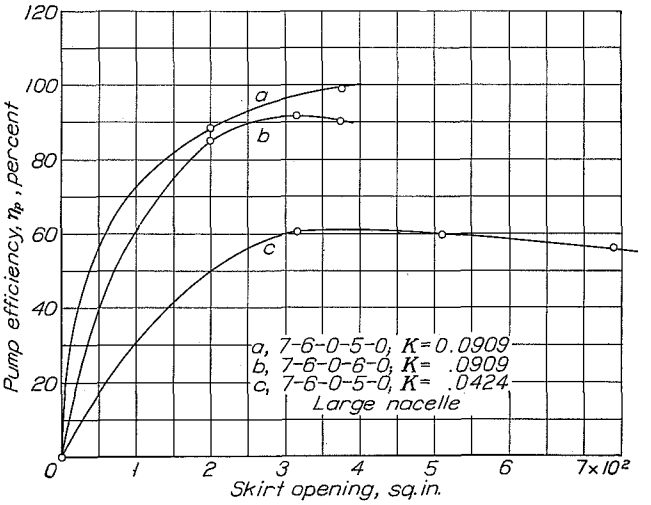

FIGURE 18.—Pump efficiency against skirt exit area.

with increase in flow velocity through the exit opening, indicating that the major loss is of the nature of mixing or impact loss occurring along the nacelle.

Figure 17 is a cross plot of figure 16, the efficiency being plotted against the conductivity, each curve representing a given skirt. Note, in particular, that the smaller skirt openings yield considerably higher efficiencies at the low conductivities corresponding to standard type baffles. The dotted curve obtained on the large nacelle 2 with a small skirt opening, shown in this figure for comparison, gives an efficiency of from 80 to 90 percent in the same range of conductivity, indicating definitely a beneficial influence from the increase in nacelle diameter.

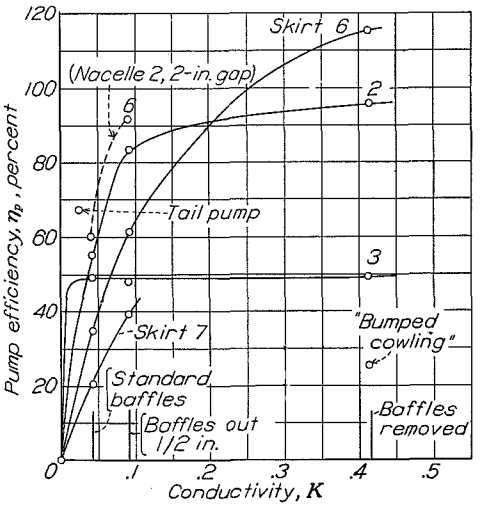

FIGURE 17.—Pump efficiency against conductivity for nose 7. Each curve is for a particular skirt.

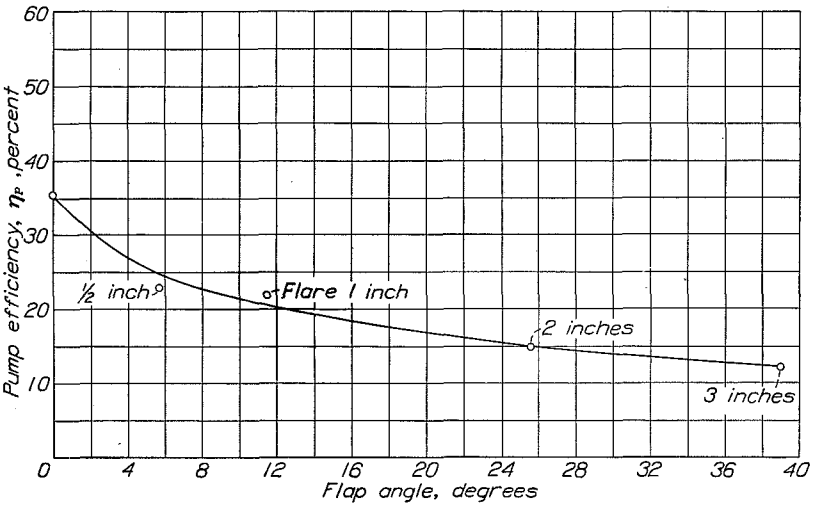

FIGURE 19.—The effect of flaps applied to skirt 8 for test arrangement 7—8—0—3—0; K=0.0424.

Figure 18 refers to the large nacelle, 2. Note that the efficiencies exceed those from the tests of the small nacelle, all lying in the range from 70 to 100 percent. These tests were obtained with skirt 6, the exit opening being varied by increasing or decreasing the actual length of the skirt. As skirt 6 is cylindrical, the exit area was varied without changing the external contour of the body.

The effect of flaps on the pump efficiency is shown in figure 19, in which the pump efficiency is plotted against the flap angle in degrees. The steep slope of the curve at small angles confirms the importance of careful streamlining in order to attain the highest efficiencies. These tests were obtained on skirt 8, which was successively bent in the shapes indicated in the main drawing (fig. 4). It is of interest to note that the available pressure drop is increased only very slightly by the flaps (table I) the maximum increase amounting to less than 20 percent and associated with a decrease in pump efficiency.

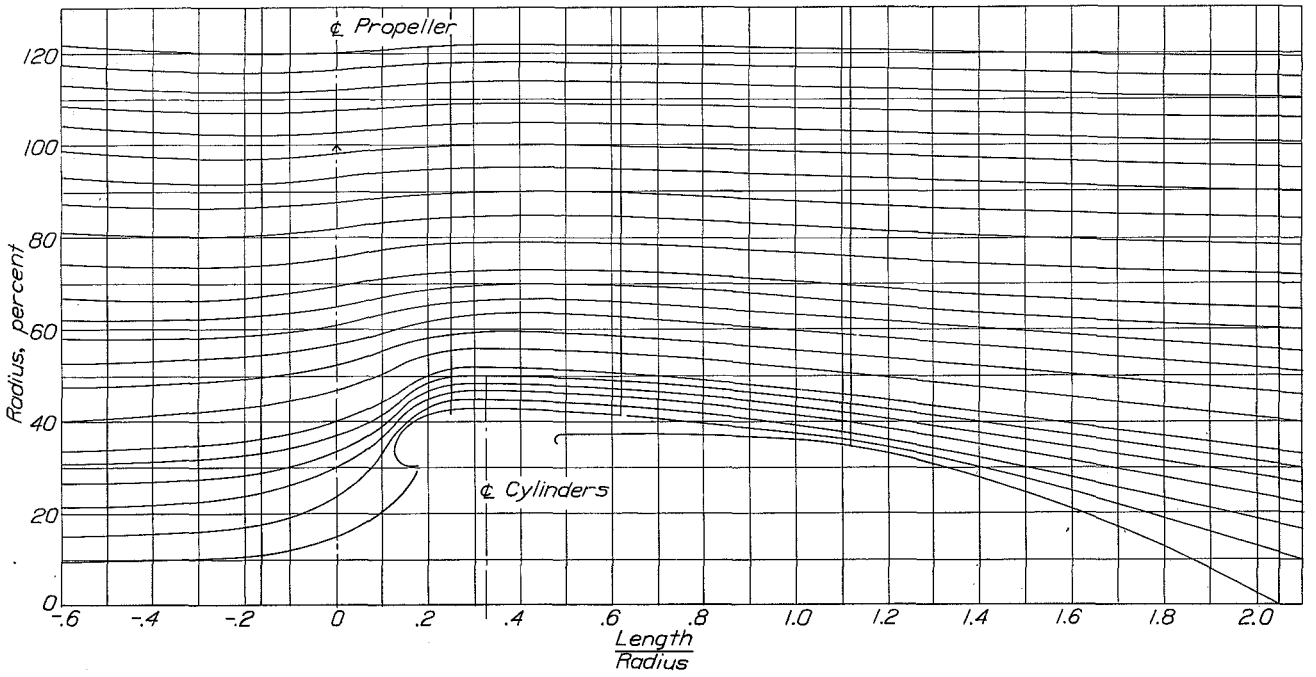

FIGURE 20.—Measured streamlines for test arrangement 7—2—B_x—3—0.

STUDY OF FLOW LINES

In order to gain a quantitative insight into the condition of the flow around and into the cowling, the actual flow lines were determined as shown in figure 20 (the method used will be described in a later paper) and a photographic study of smoke flow was carried out. Figure 21 shows a group of smoke pictures taken with a moving-picture camera. A study of these films in slow motion reveals several interesting details. There seem to exist certain fairly well-defined main flows almost stationary in character. The flow appears, on the whole, extremely turbulent with disturbances of large size. Figure 21(a) shows the flow in front of the engine. Notice the very disturbed flow. The remaining figures 21(b–e) serve to illustrate the direction of the flow lines in front of the engine and the magnitude of the conductivity. The value of the conductivity obtained from the location of the streamline outlining the flow into the cowling is in expected agreement with the calculated value; this particular streamline corresponds very nearly to the smoke line shown in figure 21(d). In figure 21(c) all the smoke flows outside, while in 21(e) all the smoke flows definitely through the cowling. Note the closeness of the smoke nozzle to the axis. These figures also demonstrate the instability of the flow around the nose of a cowling, as the smoke stream oscillates alternately in and out of the cowling.

COOLING

The photographic smoke-flow studies show a violent large-grain turbulence in front of the engine. This fact must be kept in mind when analyzing the results of the cooling tests. These results are given in compact form in the main table I. The temperatures given are the temperatures of the front and the back of the cylinder barrel. Figure 22(a) is an example of the actual distribution of the temperature around the electrically heated cylinder, the front being indicated by the 0°. This test refers to the standard baffle arrangement shown in cross section in figure 6. The temperatures plotted are the differences between the cylinder temperature and that of the tunnel air stream. The electric heat input was held constant throughout all tests at 1.75 kilowatts so that the index temperature is a direct measure of the local heat transfer. All heat-transfer tests are taken at a tunnel speed of 100 miles per hour.

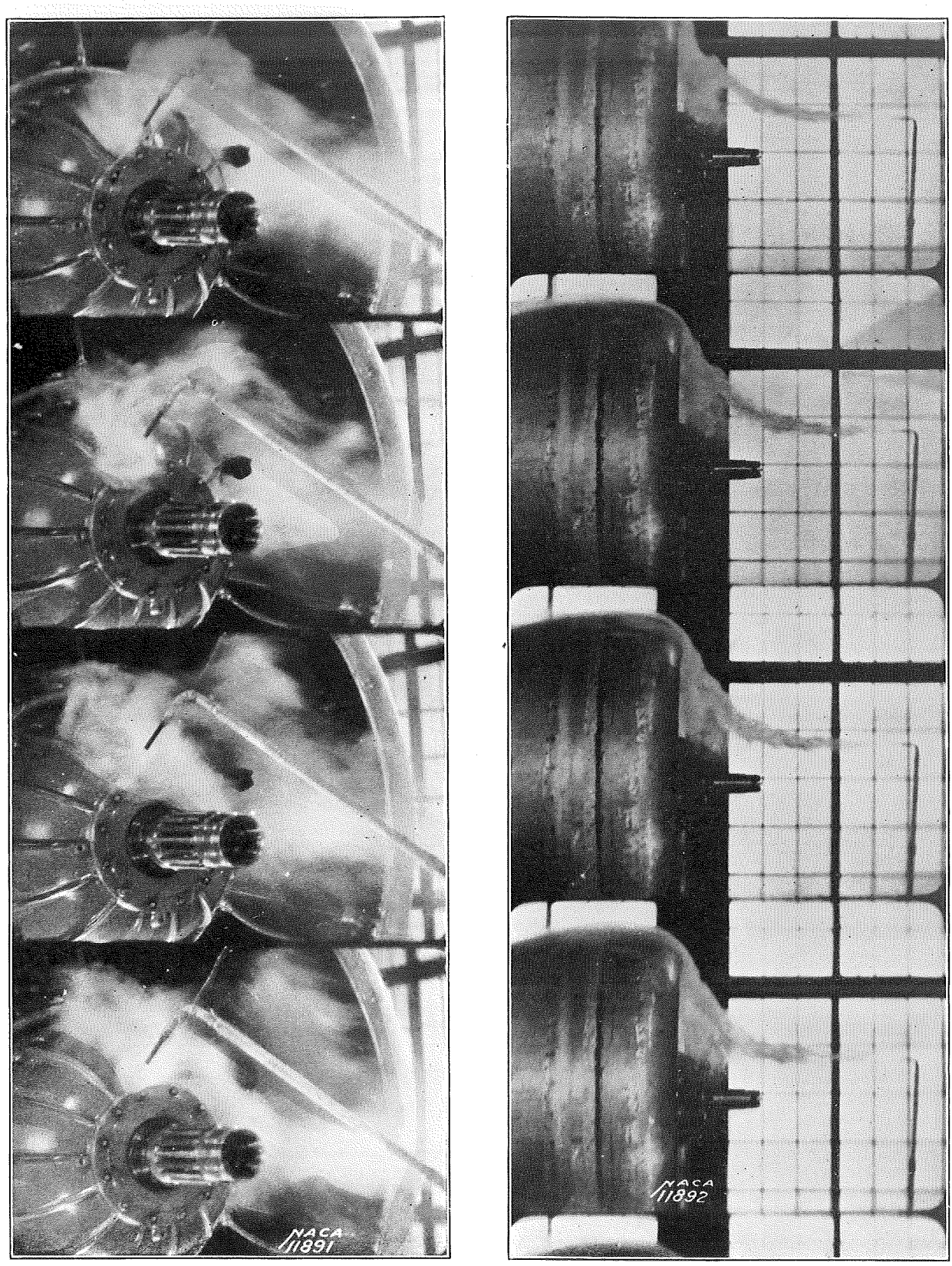

(a) Smoke flow in front of the cowling without the propeller.

(b) Smoke flow into the cowling without the propeller.

FIGURE 21.—Smoke flow around cowlings.

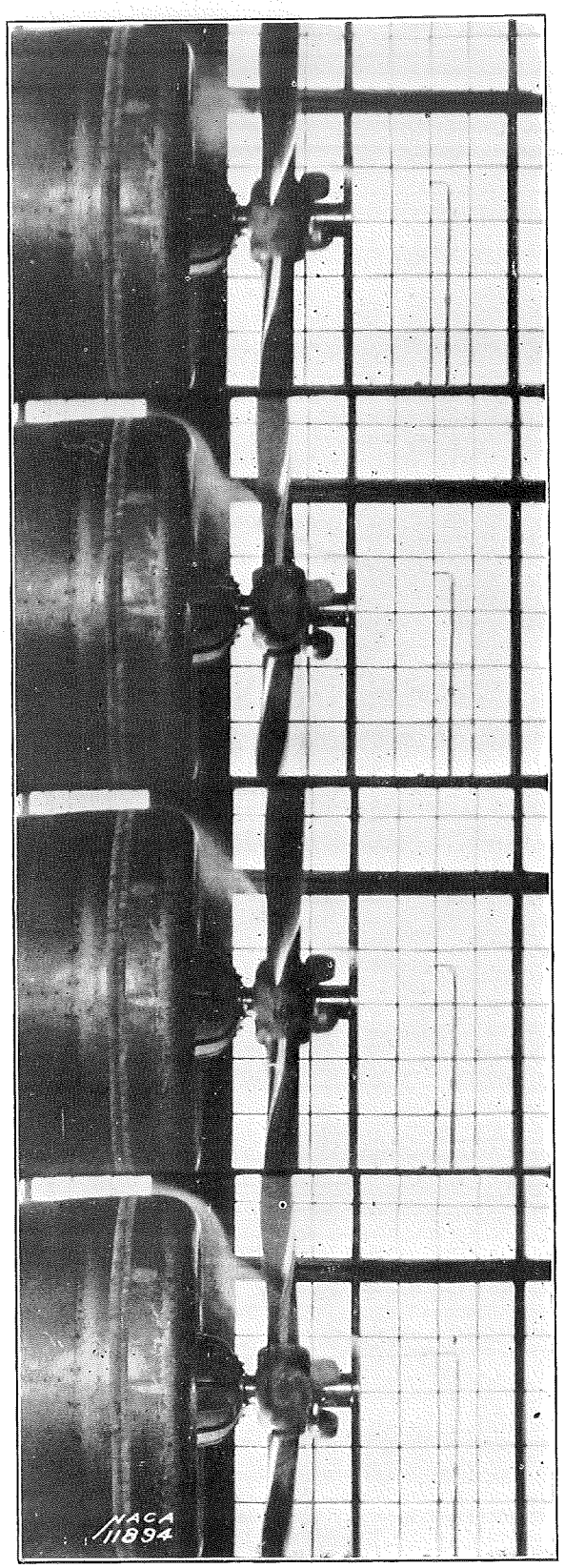

(c) Smoke flow into the cowling outside the streamline with the propeller operating.

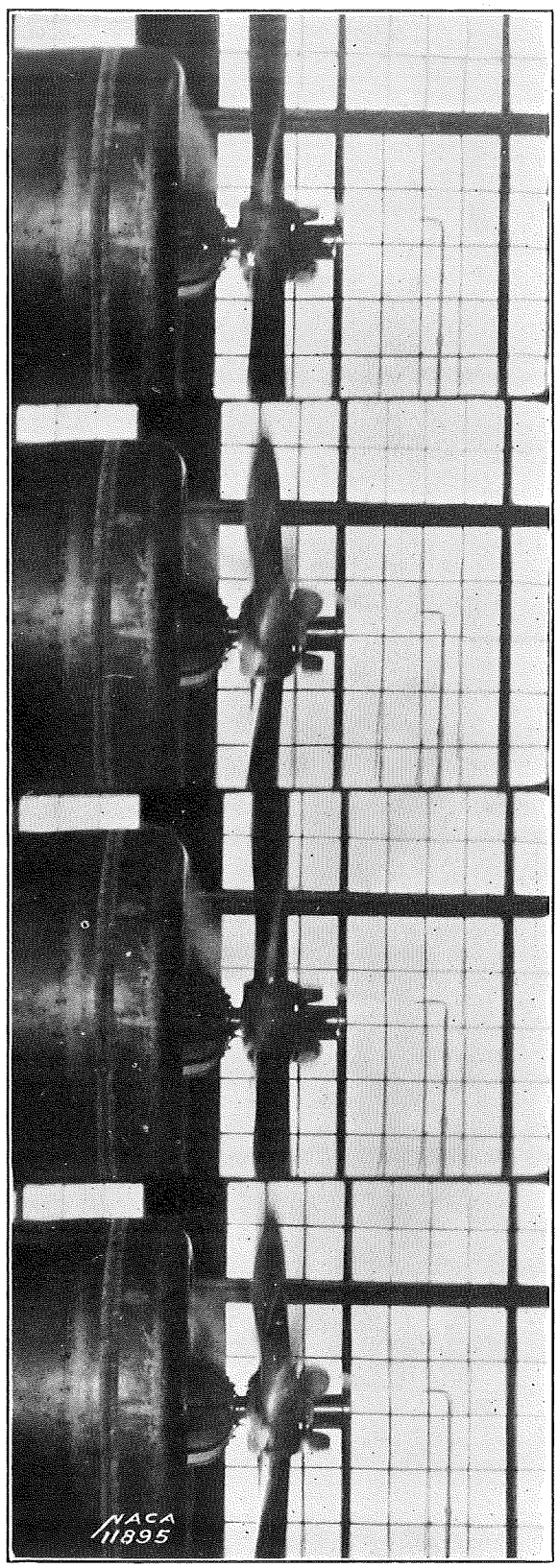

(d) Smoke flow into the cowling with the propeller operating; streamline.

FIGURE 21.—Continued. Smoke flow around cowlings.

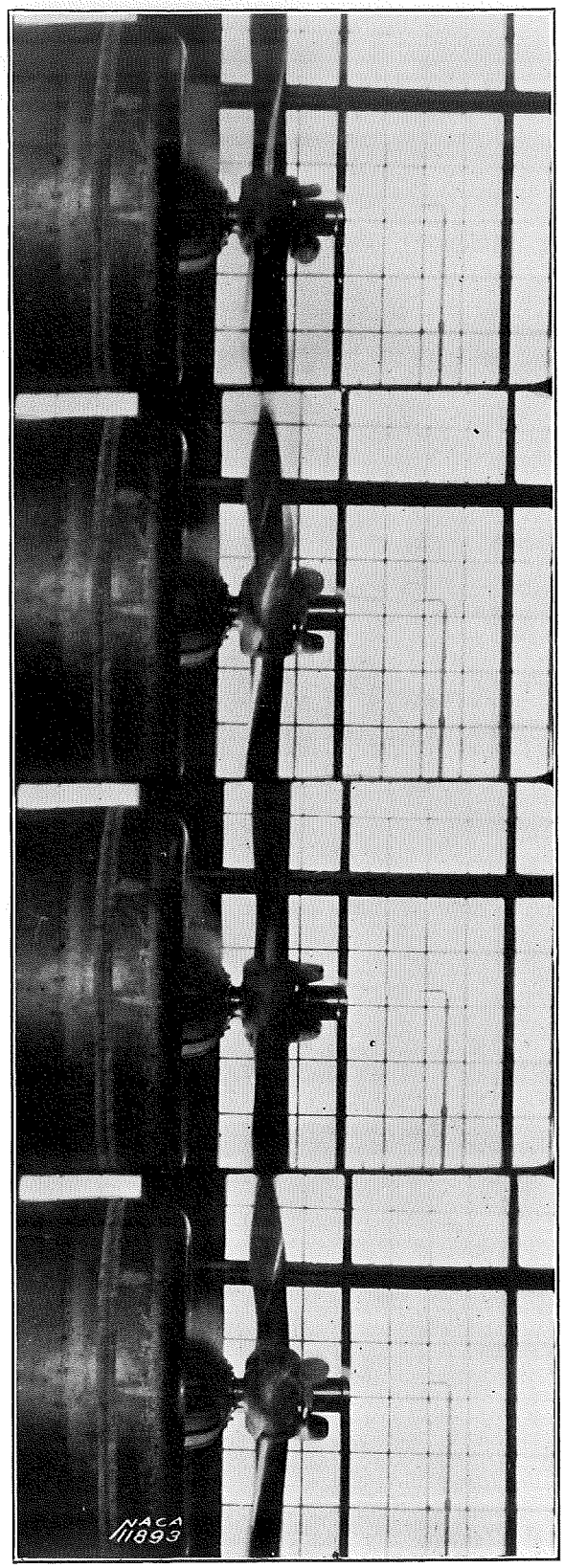

(e) Smoke flow into the cowling inside the streamline with the propeller operating.

FIGURE 21.—Continued. Smoke flow around cowlings.

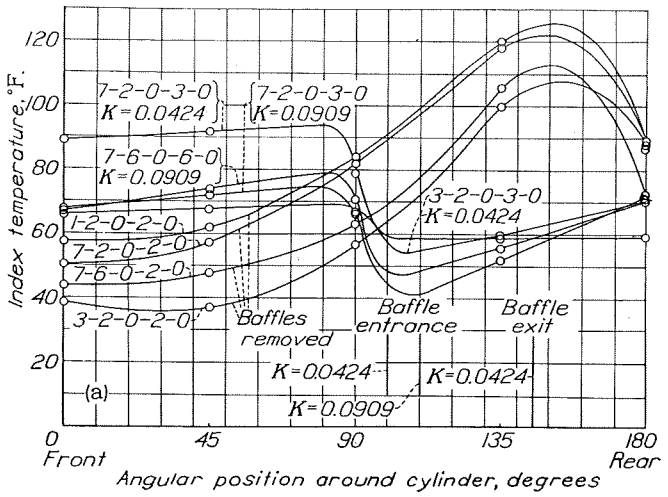

(a) Several cases with no propeller.

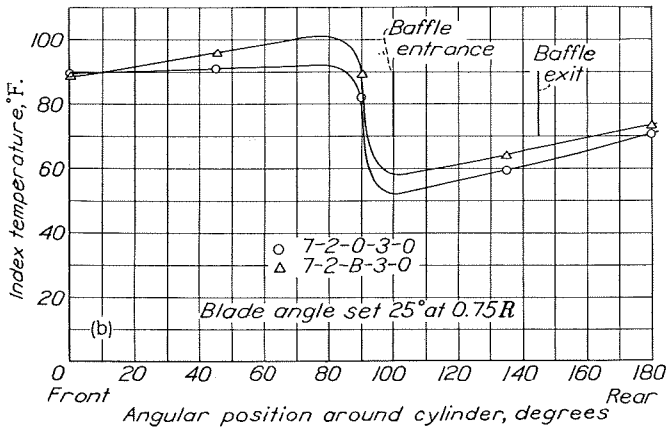

(b) Reference case with no propeller and with propeller B; $K=0.0424$.

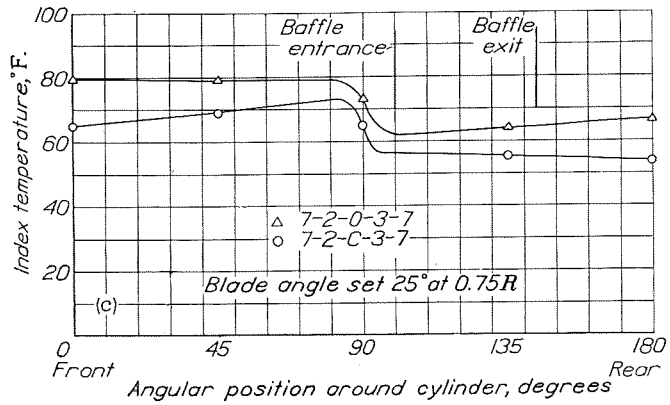

(c) Condition corresponding to most efficient cooling; $K=0.0424$.

FIGURE 22.—Temperature distribution around the electrically heated cylinder.

A reference point for the index temperatures tabulated in table I is obtained by comparing any given case with the temperatures given for the test arrangement 7—2—B—3—0, which copies an actual power run of a similar engine of 550 horsepower tested at the same tunnel velocity of 100 miles per hour and using the same external cowling arrangement. This engine

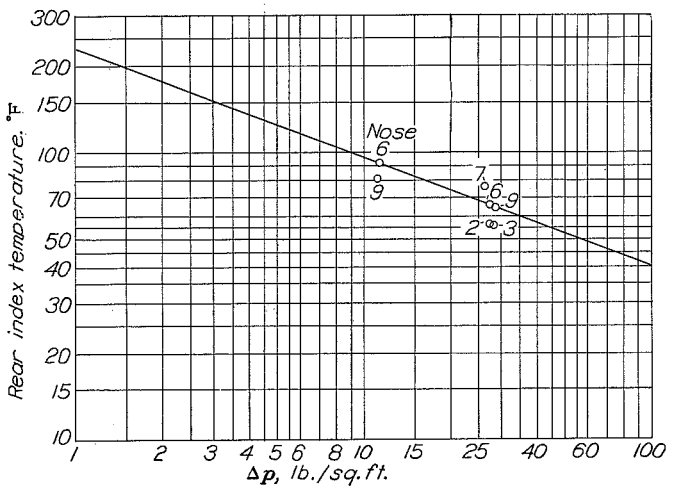

FIGURE 23.—Rear index temperature against Δp for the various noses on skirt 2; $K=0.0424$.

showed a maximum cylinder temperature of 400° F. above that of the air stream. The index temperature of 73° shown in table I for this particular test represents, therefore, exactly the same condition of cooling; that is, a rear temperature of more than 73° may be considered unsatisfactory in the same sense as a temperature in excess of 400° F. above that of the sur-

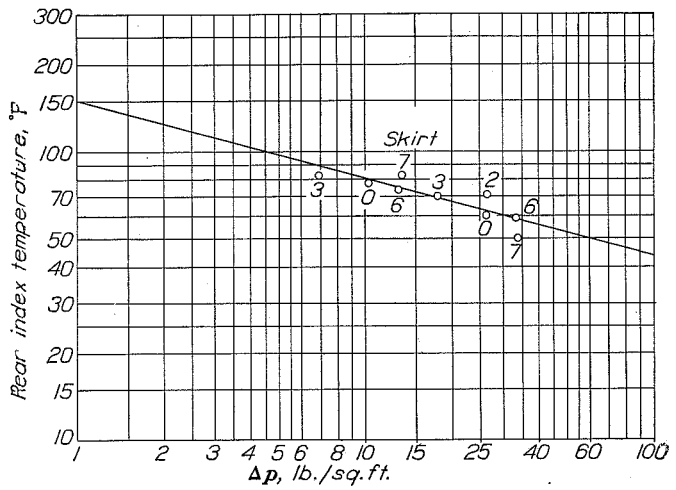

FIGURE 24.—Rear index temperature against Δp for the various skirts for nose 7 with no propeller; $K=0.0424$.

roundings in the actual case. Other plots of temperature distribution around the cylinder barrel are shown in figures 22 (b) and (c). It is to be noted that the condition constituting sufficient cooling on the Pratt & Whitney Wasp S1H1–G might be too conservative. It is entirely possible that a reference temperature of 80° F. or even of 90° F. might represent sufficient cooling on improved designs.

Figures 23, 24, 25, and 26 illustrate the dependency of the rear index temperature on the pressure drop across the engine, plotted on logarithmic scales. The slope of the line that seems to fit the experimental results the closest is -0.31, or $T_1=C\Delta p^{-0.31}$. Figure 23 shows results for the various nose shapes using skirt 2 and no propeller; figure 24, the results for various

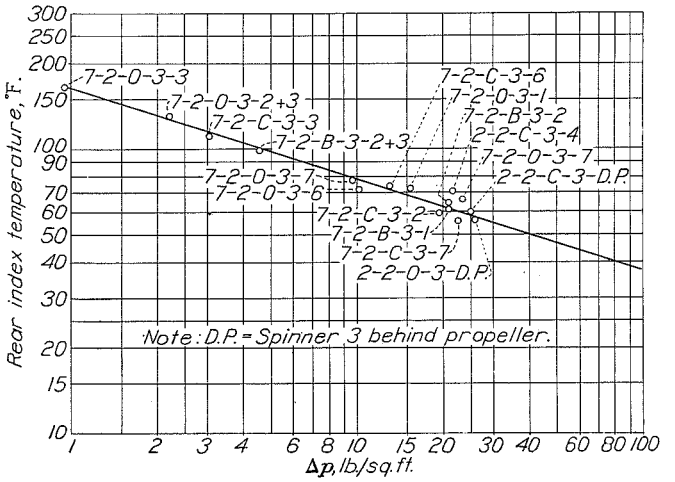

FIGURE 25.—Rear index temperature against Δp for the various spinners on noses 2 and 7 with skirt 2; $K=0.0424$.

skirts in conjunction with nose 7; figure 25 gives the results for a number of combinations of propellers and spinners on noses 2 and 7; and figure 26 shows the results for the conductivity 0.0909 both for the large and the small nacelles. Two main conclusions may be drawn from these results:

(1) That the rear index temperature for a given conductivity depends only on the pressure drop through

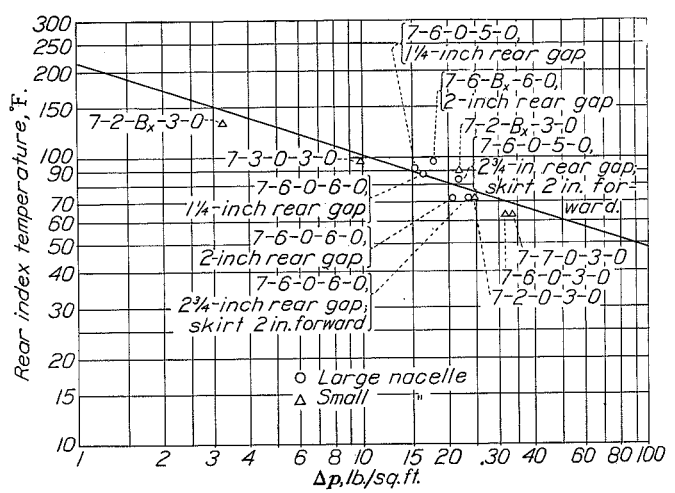

FIGURE 26.—Rear index temperature against Δp for several arrangements; $K=0.0909$.

the baffle. All points lie reasonably close to the average line drawn in the figures.

(2) That the increased conductivity has a detrimental effect on the heat transmission. It is seen by comparing the results in figures 25 and 26 representing the conductivities of 0.0424 and 0.0909, respectively, that the temperature is increased from 78° F. to 102° F. at a given pressure drop of $\Delta p=10$ pounds per square foot.

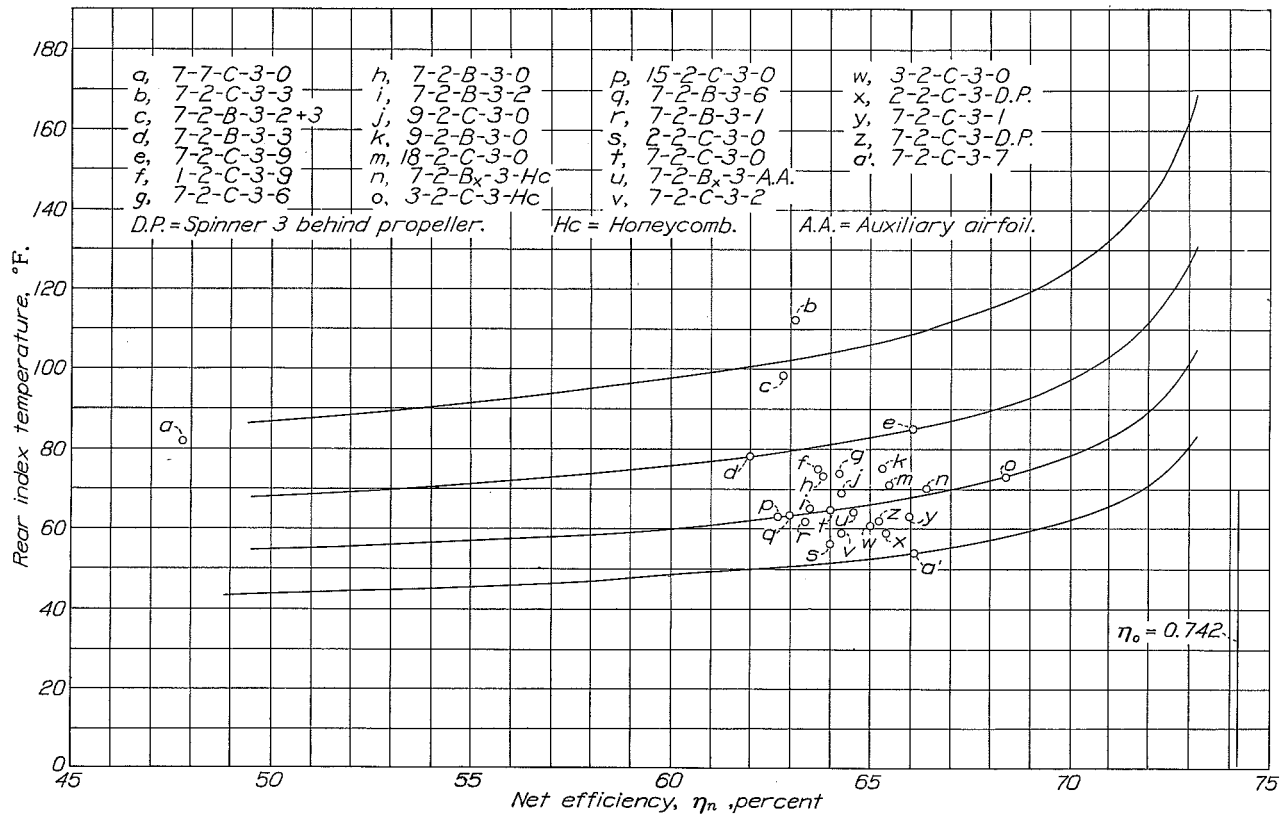

FIGURE 27.—Rear index temperature against η_n for all cases of 0.0424 conductivity with curves designating equal performance in respect to cooling and efficiency. Small nacelle used.

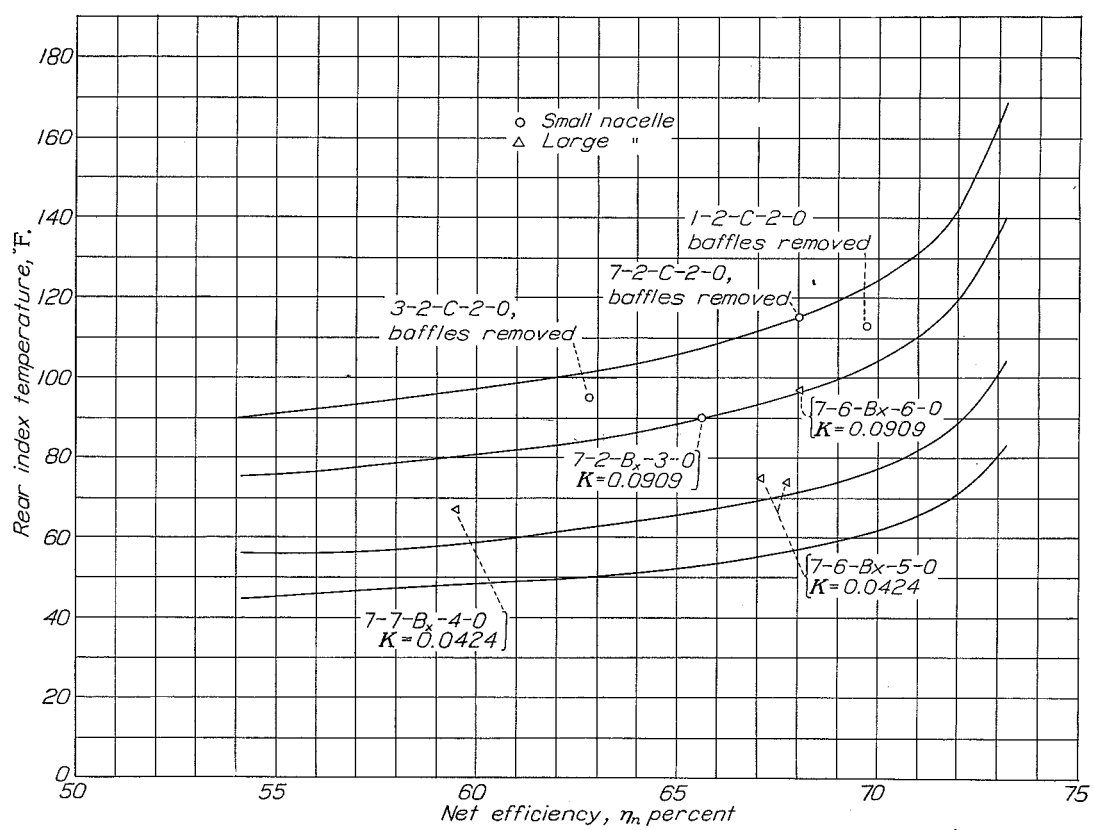

FIGURE 28.—Rear index temperature against net efficiency.

In figures 27 and 28 the index temperature is plotted against the net efficiency η_n, in figure 27 for the standard conductivity $K=0.0424$ and the small nacelle, and in figure 28 for the large conductivity $K=0.0909$ for tests on both the small and large nacelles. These charts give in a compact form the entire results of this investigation. The cost of the cooling is represented by the distance between the particular point η_n and the ordinate representing the ideal efficiency at $\eta_0=74.2$ percent. The temperatures are seen to range from 54° F. to more than 100° F. The curves drawn in the figures are considered to be curves of constant performance. They are obtained by the following reasoning: If overcooling exists in a certain test, there is a possible and permissible gain in the net efficiency, which can be realized by using a narrower skirt. Assuming a constant pump efficiency there exist the following relations:

The index temperature $T_i=\Delta p^{-0.31}$ constant and the work done $\eta_0-\eta=\Delta p^{3/2}$ constant and thus, by elimination of Δp, $T_i=(\eta_0-\eta_n)^{-0.206}$ constant or T_i is nearly proportional to the inverse of $\sqrt[5]{\eta_0-\eta_n}$. Thus it is seen that the change in T_i due to a regulation in the quantity of cooling air can be predicted on the basis of the net efficiency. A given increase in index temperature is thus associated with a definite increase in net efficiency.

Although the rear cylinder temperatures seem to depend in a very regular manner on the pressure drop Δp, the front temperature shows no such relationship. It is rather remarkable that the front portion of the cylinders cools, on the whole, just as well as the baffled portion. The very unstable three-dimensional flow in front of the cowling is obviously very beneficial to the heat transmission. As the present investigation is restricted primarily to the matter of cowling design, only a few remarks will be made here. It is noted (fig. 22(a)) that an unbaffled engine is overcooled on the front and overheated on the rear, demonstrating conclusively the technical value of the baffles. A comparison of figures 22(b) and (c) shows the apparent value of a spinner in improving the frontal heat transmission. A study of the main table I reveals several cases of good front cooling. Spinner 3 appears to show a very low front temperature.

In regard to the cost of the cooling on the front, it is observed in table I that the drag of the basic cowling shape is 42 pounds at 100 miles per hour and that the drag of the better streamline form employing nose 8 is only 32 pounds. It seems necessary to conclude that the difference of 10 pounds represents the cost of the comparatively poor aerodynamic shape of the nose of the conventional type cowling, which, on the other hand, reappears as a beneficial effect in regard to the cooling of the front of the cylinders. It might be expected that the reasonably large spinner might reclaim a certain fraction, at least, of the 10-pound drag loss. The various spinners tested have been described (fig. 9). It is quite interesting to observe that several of these spinners show a large beneficial influence on the front cooling, particularly the flat spinners 1, 3, and 6.

Table II shows the front temperatures obtained on various spinners.

Figure 29 shows the pressure distribution obtained on nose 7 in the presence of three typical spinners. In this group the plot (b) for spinner 7 is of the most interest, owing to the fact that this test represents the most efficient arrangement obtained throughout the entire series. (Cf. fig. 27.) The high net efficiency and the good cooling are in this case definitely attributable to the spinner. The relatively small dimensions of this spinner make possible the practical realization of these gains.

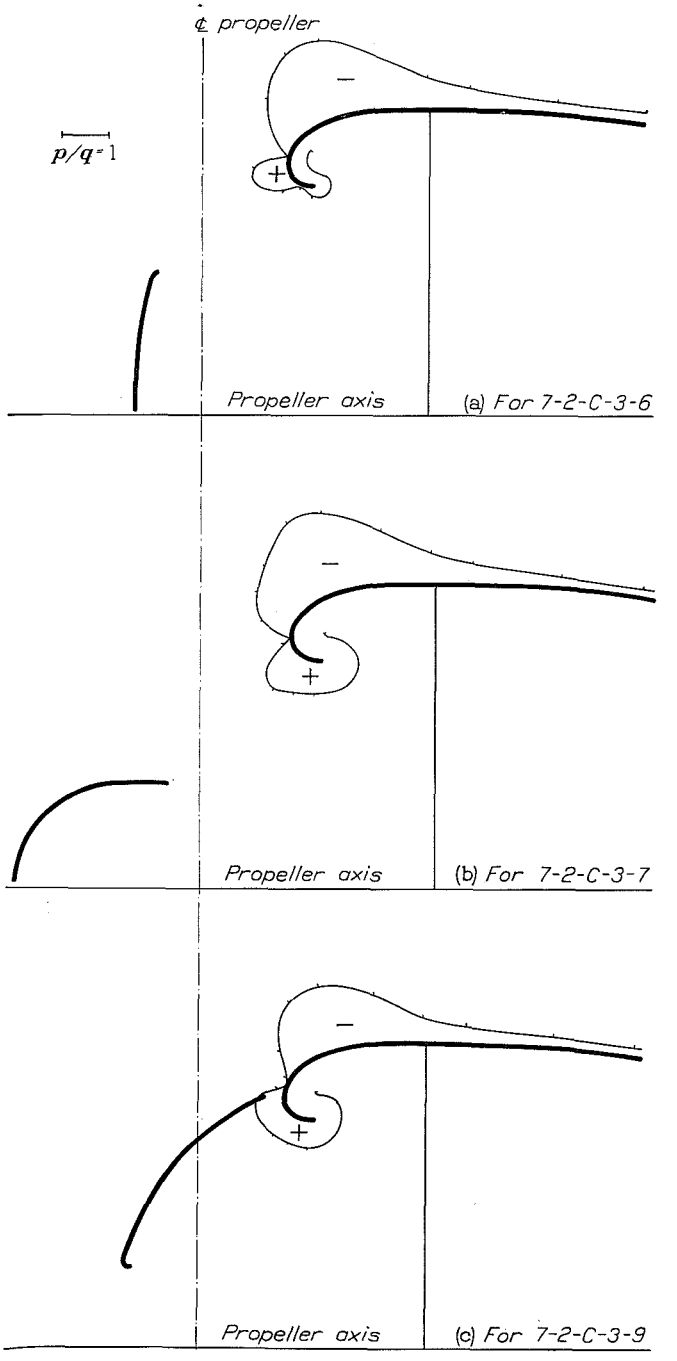

FIGURE 29.—The pressure distribution as affected by several spinners.

There is, finally, another problem that will be touched upon. It concerns the matter of baffle design. The present investigation confined itself to tests on a single baffle as described. Pitot tubes installed between the fins of the cylinder permitted the determination of the energy loss along the flow path. Results obtained in parallel with the temperature curves just presented (in fig. 22) are given for the total pressures in figure 30. Figure 30(a) shows these curves for the two lowest conductivities. It may be seen in figure 6 that the baffle covers about 45°, extending from 100° to 145° for the tightly fitting baffle. It is interesting so observe that only about one-third of the energy lost takes place inside the baffle and two-thirds behind. The baffle transposed rearward one-half inch and forming a diverging channel appears to provide a more efficient design, the exit loss being fairly small. The next figure 30(b) shows several cases with baffles removed. The low pressure in front of the cylinder with nose 3 is rather noticeable. The standard baffle is shown again in figure 30(c). Notice the slight effect of the propeller. Figure 30(d) is of interest as it refers to the test arrangement 7—2—C—3—7, which represents in every respect the best combination discovered in the investigation.

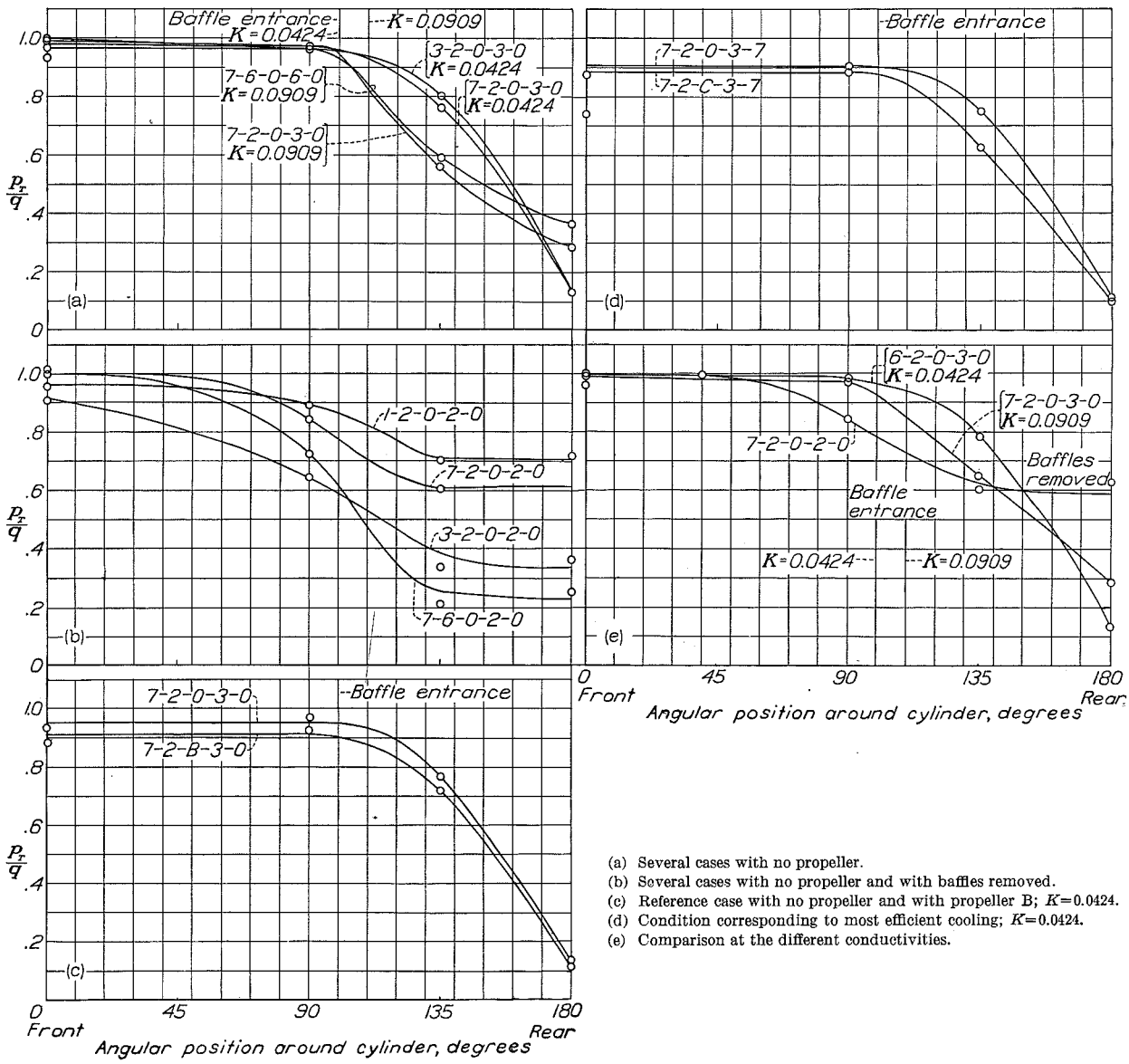

(a) Several cases with no propeller.
(b) Several cases with no propeller and with baffles removed.
(c) Reference case with no propeller and with propeller B; $K=0.0424$.
(d) Condition corresponding to most efficient cooling; $K=0.0424$.
(e) Comparison at the different conductivities.

FIGURE 30.—Total pressure distribution around the cylinder.

GENERAL CONCLUSIONS

1. It has been found that the basic blunt-nose cowling shape of an air-cooled engine has a drag somewhat in excess of that of a more properly streamline shape, such as an airship form. It was shown that the blunt nose is the cause of an instability in the air flow in front of the cowling that sets up a large-scale turbulence. This turbulence accounts for the remarkably good cooling on the front of the engine. The mechanical cost of this particular cooling compares favorably with the pressure cooling obtained on the rear of the engine.

2. The pumping efficiency, the ratio of the internal work done to the work expended by the corresponding increase in drag, has been found to range from almost zero to more than unity. The pump efficiency is largely dependent on the flow velocity and the shape of the exit passage.

3. The leading edge of the cowling should be given a smooth, very rounded form, such as nose 7. The diameter of the cowling inlet nose opening was found to be of little significance, either in regard to drag or in regard to cooling. As a general rule, the larger the opening, the better, care being taken only to provide a proper design of the nose contour. In this connection, it is worth keeping in mind that the flow immediately in front of the cowling is almost radial. A too straight cowling gives rise to a condition of breakdown of the flow at the front edge of the cowling. This effect was demonstrated in the present investigation in the case of cowling 1.

4. It has been found that a smooth contour line for the skirt design is a primary requirement. The rear edge of the skirt should not project into the air stream. The necessary exit opening should be obtained by a retraction of the inner cowling. The design of the inner cowling is less critical.

5. The most obvious method of varying the pressure across the engine is to vary the area of the exit opening. If this increase in area is accompanied by an outward flare of the trailing edge as is accomplished by the use of cowl flaps, a slightly greater increase in the pressure difference can be obtained than that resulting from a simple increase in area.

6. It is obvious from theoretical considerations that in a normal cruising condition the propeller causes only a slight contraction of the streamlines around the nacelle and that therefore no important effects of any kind are to be expected. This effect was amply verified by the test results. The propeller actually shows a blocking effect that gives a slight decrease in cooling. Spinners influence the stability of the flow around the front of the cowling and do, in some cases, improve the over-all performance of the combination. Spinner 7 on cowling 7 showed both an increase in net efficiency and improved cooling. The condition at low air speed is discussed in reference 9.

7. Tests performed on the combination with the larger afterbody showed a consistent increase in performance, demonstrating the importance of a smooth merging of the contour lines of the front and afterbody and the value of a better exposure of the exit opening of the unexpanded and stabler air stream.

8. The main result of the cooling problem studied in this investigation is that a tightly baffled engine is definitely superior in regard to cooling efficiency. The results obtained at the minimum conductivity $K=0.0424$ are in every respect better than those obtained at the conductivity $K=0.0909$ or on an unbaffled engine. Another important result is the observation that the inherent large-scale turbulence occurring in front of the cowling accounts for the good cooling on the exposed frontal area of the engine. This effect should, of course, be used to the fullest extent in the design of baffles.

9. It is of interest to note that, although increased conductivity of an engine is beneficial to pump efficiency, the detrimental effect on cooling is so much greater that no compromise is possible. In other words, a tightly baffled engine is superior in over-all performance in spite of an inferior pumping efficiency. With a new type of nose-slot cowling greater pump efficiency is obtained at low conductivities.

LANGLEY MEMORIAL AERONAUTICAL LABORATORY,
NATIONAL ADVISORY COMMITTEE FOR AERONAUTICS,
LANGLEY FIELD, VA., *May 18, 1936.*

LIST OF SYMBOLS

p_f, pressure in front of the engine.

p_r, pressure in rear of the engine.

Δp, pressure drop across the engine, $\Delta p = p_f - p_r$.

D, drag of the cowling-nacelle unit.

D_0, drag of a smooth nacelle entirely enclosing the engine.

q, dynamic pressure of the air stream.

ρ, density of the air.

F, frontal area of the engine.

$C_D = \frac{D}{qF}$

$C_{D_0} = \frac{D_0}{qF}$

Q, quantity of the air flowing through the cowling.

V, velocity of the air stream.

$\eta_p = \frac{Q\Delta p}{(D-D_0)V}$, pump efficiency, without propeller.

R, net force on the thrust balance with propeller on.

$T = R + D$, propulsive thrust.

P, power supplied to propeller.

$\eta_n = \frac{RV}{P}$, net efficiency of propeller-nacelle unit.

S, propeller disk area.

$P_c = \frac{P}{qSV}$, unit disk loading.

$\frac{1}{\sqrt[3]{P_c}} = V\sqrt[3]{\frac{\rho S}{2P}}$

η_0, net propeller-nacelle efficiency obtained on same set-up as used for D_0.

$\eta_p = \frac{Q\Delta p}{(\eta_0 - \eta_n)P}$, pump efficiency with propeller operating.

A, area of the free air stream entering the cowling.

$k = \frac{A}{\sqrt{\frac{\Delta p}{q}}}$

$K = \frac{k}{F} = \frac{\frac{A}{F}}{\sqrt{\frac{\Delta p}{q}}}$, conductivity of the engine.

$Q = K\sqrt{\frac{\Delta p}{q}}FV$

p_2, static pressure at the exit of the slot.

V_2, velocity in the exit of the slot.

Δp_2, pressure drop through exit passage.

A_2, area of exit of the slot.

$\Delta P = \Delta p + \Delta p_2$, total pressure drop across cowling.

K_2, apparent conductivity of the exit slot.

$\frac{\Delta P}{q} = \left(\frac{Q}{FV}\right)^2\left[\frac{1}{K^2} + \frac{1}{K_2^2}\right]$, relation of conductivities of engine and slot exit.

n, revolutions per second of the propeller.

D, diameter of the propeller.

$C_T = \frac{T}{\rho n^2 D^4}$, thrust coefficient.

$C_P = \frac{P}{\rho n^3 D^5}$, power coefficient.

$\frac{V}{nD}$, advance-diameter ratio of the propeller.

$\eta = \frac{TV}{P}$, propulsive efficiency.

T_i, index temperature.

W, work done by the cooling air.

REFERENCES

1. Weick, Fred E.: Drag and Cooling with Various Forms of Cowling for a "Whirlwind" Radial Air-Cooled Engine—I. T. R. No. 313, N. A. C. A., 1929.
2. Weick, Fred E.: Drag and Cooling with Various Forms of Cowling for a "Whirlwind" Radial Air-Cooled Engine—II. T. R. No. 314, N. A. C. A., 1929.
3. Schey, Oscar W., and Biermann, Arnold E.: The Effect of Cowling on Cylinder Temperatures and Performance of a Wright J-5 Engine. T. R. No. 332, N. A. C. A., 1929.
4. McAvoy, William H., Schey, Oscar W., and Young, Alfred W.: The Effect on Airplane Performance of the Factors that Must Be Considered in Applying Low-Drag Cowling to Radial Engines. T. R. No. 414, N. A. C. A., 1932.
5. Theodorsen, Theodore: On the Theory of Wing Sections with Particular Reference to the Lift Distribution. T. R. No. 383, N. A. C. A., 1931.
6. Goldstein, Sydney: On the Vortex Theory of Screw Propellers. Proc. Roy. Soc. (London), Series A, vol. 123, April 6, 1929, pp. 440–465.
7. Weick, Fred E., and Wood, Donald H.: The Twenty-Foot Propeller Research Tunnel of the National Advisory Committee for Aeronautics. T. R. No. 300, N. A. C. A., 1928.
8. Theodorsen, Theodore, Stickle, George W., and Brevoort, M. J.: Characteristics of Six Propellers Including the High-Speed Range. T. R. No. 594, N. A. C. A., 1937.
9. Theodorsen, Theodore, Brevoort, M. J., and Stickle, George W.: Cooling of Airplane Engines at Low Air Speeds. T. R. No. 593, N. A. C. A., 1937.
10. Theodorsen, Theodore, Brevoort, M. J., Stickle, George W., and Gough, M. N.: Full-Scale Tests of a New Type N. A. C. A. Nose-Slot Cowling. T. R. No. 595, N. A. C. A., 1937.
11. Hartshorn, A. S.: Wind Tunnel Investigation of the Cooling of an Air-Jacketed Engine. R. & M. No. 1641, British A. R. C., 1935.

TABLE I.—CONDENSED EXPERIMENTAL RESULTS

1	2	3	4	5	6	7	8	9	10	Remarks
Designation of arrangement (Nose / Skirt / Propeller / Inner cowling / Spinner)	$p_f q$	$p_r q$	(2—3) $\Delta p/q$	C_D (D/qF)	Drag in lb. at q=25.6 lb. per sq. ft., or thrust at $1/\sqrt[3]{P_c}$=1.8 and q=25.6 lb. per sq. ft.	η_n at $1/\sqrt[3]{P_c}$=1.8	η_p	Index temperatures: Front T_f	Index temperatures: Rear T_r	
NACELLE 1—ZERO AIR										
2— 5—0 —3—0				0.1193	45.0					Closed skirt.
7— 2—0 —3—0	1.00	−0.274	1.274	.1365	51.5					Closed by flat plate at front of cylinders.
7— 3—0 —3—0	1.00	−.071	1.071	.1246	47.0					
7— 6—0 —3—0	1.00	−.417	1.417	.1749	66.0					
7— 7—0 —3—0	1.00	−.442	1.442	.245	92.5					
7— 0—0 —3—0	1.00	−.371	1.371	.1616	61.0					
STANDARD BAFFLES—CONDUCTIVITY 0.0424										
0— 2—0 —3—0	1.004	−.295	1.299	1.182	446.0		0.058			
0— 2—C —3—0	.910	−.230	1.140			−0.075	.068			
1— 2—0 —3—0	1.008	−.062	1.070	.330	124.5		.214			
1— 2—B —3—0	.982	−.050	1.032		206.0	.589	.316			
1— 2—C —3—0	.906	−.059	.965		211.0	.605	.320			
2— 2—0 —3—0	.956	−.048	1.004	.194	73.0		.517	81.7	57.1	
2— 2—B —3—0	.926	−.057	.983		222.0	.636	.421			
2— 2—C —3—0	.883	−.057	.939		223.0	.640	.412	71.6	56.2	
2— 5—0 —3—0				.123	46.4					Zero cooling air.
3— 2—0 —3—0	.973	−.051	1.024	.196	74.0		.521	66.0	57.0	
3— 2—B —3—0	.877	−.061	.939		226.0	.648	.445			
3— 2—C —3—0	.853	−.062	.915		227.0	.650	.438	59.8	60.8	
4— 2—0 —3—0	.989	−.039	1.027	.1935	73.0		.539			
4— 2—B —3—0	1.004	−.032	1.036		214.0	.612	.375			
4— 2—C —3—0	.894	−.045	.944		218.0	.625	.363			
5— 4—0 —2—0	.984	−.064	.920	.1755	66.4		.823			Conductivity 0.060. Preliminary test.
6— 2—0 —3—0	.971	−.058	1.030	.2027	76.5		.486	79.3	65.9	
6— 2—B —3—0	.885	−.061	.945		224.0	.642	.423			
6— 2—C —3—0	.868	−.074	.942		220.0	.631	.380			
6— 3—0 —3—0	.962	.345	.616	.1603	60.5		.417	81.8	68.8	
6— 4—0 —2—0	.960	.047	.913	.1755	66.4		.813			Do.
7— 2—0 —3—0	.983	−.046	1.030	.1929	72.5		.551	89.5	70.6	
7— 2—B —3—0	.901	−.053	.954		223.0	.638	.410	88.6	73.0	
7— 2—C —3—0	.871	−.062	.933		223.0	.640	.408	77.2	64.7	
7— 2—B_x—3—0	.888	−.045	.934		226.0	.646	.432			
7— 3—0 —3—0	.946	.358	.588	.1497	56.5		.494	104.6	76.5	
7— 4—0 —2—0	.952	.067	.885	.1772	67.0		.757			Do.
7— 6—0 —3—0	.975	−.218	1.194	.2700	102.0		.349	82.0	59.0	
7— 7—0 —3—0	.967	−.249	1.215	.387	146.0		.205	71.3	50.7	
7— 7—C —3—0	.871	−.312	1.183		167.0	.478		81.0	81.7	
7— 0—0 —3—0	.953	−.261	1.214	.237	89.5		.451	81.5	60.0	
FLAPS										
7— 8—0 —3—0	0.956	−0.222	1.179	0.265	100.0		0.353			
7— 8—C —3—0	.870	−.264	1.133		201.0	0.576	.336			
7— 8—0 —3—0	.980	−.233	1.213	.307	116.0		.289			½-inch flare.
7— 8—C —3—0	.877	−.293	1.170		186.0	.534	.280			Do.
7— 8—0 —3—0	.972	−.242	1.214	.372	140.5		.218			1-inch flare.
7— 8—C —3—0	.874	−.319	1.193		170.0	.486	.235			Do.
7— 8—0 —3—0	.995	−.246	1.241	.506	191.0		.149			2-inch flare.
7— 8—C —3—0	.872	−.289	1.161		108.0	.310	.134			Do.
7— 8—0 —3—0	.980	−.246	1.225	.583	220.0		.122			3-inch flare.
7— 8—C —3—0	.874	−.291	1.165		73.0	.208	.109			Do.
STREAMLINE SHAPE										
8— 3—0 —2—0				0.1007	38.0					Zero cooling air.
8— 5—0 —2—0				.0861	32.5					Do.
9— 2—0 —3—0	0.959	−0.058	1.017	.1987	75.0		0.497	73.0	64.0	
9— 2—B —3—0	.842	−.077	.919		228.0	0.653	.456	74.0	75.0	
9— 2—C —3—0	.836	−.080	.916		224.0	.643	.408	68.0	69.0	
NOSE TO FIT BLOWER										
15— 2—0 —3—0	0.984	−0.031	1.015	0.1975	74.5		0.500	99.0	60.5	
15— 2—C —3—0	.893	−.044	.937		219.0	.627	.364	95.0	63.0	
PERFORATED DISK										
18— 2—0 —3—0	0.793	−0.074	0.867	0.1908	72.0		0.429			
18— 2—B —3—0	.768	−.083	.851		223.0	0.640	.354			
18— 2—C —3—0	.692	−.086	.778		229.0	.655	.365	110.0	71.0	
FLAT DISK										
19— 2—0 —3—0		−0.300		0.1259	47.5					Zero cooling air.
19— 5—0 —3—0				.1115	42.0					Zero cooling air. (C_{D_0}).
19— 5—B —3—0					254.0	0.728				Zero cooling air.
19— 5—C —3—0					259.0	.742				Zero cooling air. (η_0).

TABLE I.—CONDENSED EXPERIMENTAL RESULTS—Continued

1	2	3	4	5	6	7	8	9	10	Remarks
Designation of arrangement (Nose—Skirt—Propeller—Inner cowling—Spinner)	p_f/q	p_r/q	(2−3) $\Delta p/q$	C_D (D/qF)	Drag in lb. at q=25.6 lb. per sq. ft., or thrust at $1/\sqrt[3]{P_c}$=1.8 and q=25.6 lb. per sq. ft.	η_n at $1/\sqrt[3]{P_c}$=1.8	η_p	Index temperatures: Front T_f	Index temperatures: Rear T_r	
SPINNERS										
1— 2—0 —3—1	0.598	−0.085	0.683	0.1855	70.0		0.321			Position 1.
1— 2—C —3—1	.674	−.071	.745		215.0	0.617	.237			Do.
1— 2—0 —3—1	.437	−.103	.540	.1841	69.5		.232			Position 2.
1— 2—0 —3—2	.707	−.074	.781	.1975	74.5		.339			
1— 2—C —3—2	.723	−.073	.796		214.0	.612	.252			
1— 2—C —3—9	.743	−.071	.814		222.0	.637	.323	83.0	75.0	
2— 2—0 —3—3	.895	−.062	.957	.1895	71.5		.504	84.0	56.0	Dishpan.
2— 2—C —3—3	.832	−.071	.903		228.0	.654	.452	78.0	59.0	Do.
7— 2—0 —3—1	.481	−.088	.569	.1815	68.5		.256	72.5	66.0	Position 1.
7— 2—B —3—1	.673	−.070	.743		221.0	.634	.272	59.0	62.0	Do.
7— 2—C —3—1	.547	−.087	.634		230.0	.660	.284	65.0	63.0	Do.
7— 2—0 —3—2	.548	−.069	.617	.1815	68.5		.291			
7— 2—B —3—2	.677	−.066	.743		222.0	.635	.275	67.0	65.0	
7— 2—C —3—2	.608	−.084	.692		224.0	.643	.268	62.0	59.0	
7— 2—0 —3—3	−.176	−.210	.034	.1550	58.5		.006	112.0	158.0	
7— 2—B —3—3	−.028	−.178	.150		216.0	.620	.022	50.0	78.0	
7— 2—C —3—3	−.087	−.194	.107		220.0	.631	.015	68.0	112.0	
7— 2—C —3—3	.671	−.082	.753		228.0	.652	.334	82.0	62.0	Dishpan.
7— 2—0 —3—2&3	−.126	−.206	.080	.1510	57.0		.024	87.0	128.0	
7— 2—B —3—2&3	.009	−.177	.186		219.0	.628	.032	65.0	98.0	
7— 2—0 —3—6	.254	−.121	.375	.1722	65.0		.159	69.5	74.0	
7— 2—B —3—6	.431	−.106	.537		220.0	.630	.161	55.0	63.0	
7— 2—C —3—6	.351	−.117	.468		224.0	.642	.148	66.0	74.0	
7— 2—0 —3—7	.778	−.070	.848	.1935	73.0		.400	80.0	67.0	
7— 2—C —3—7	.744	−.065	.809		231.0	.661	.413	65.0	54.0	
7— 2—C —3—9	.199	−.145	.344		231.0	.661	.115	55.0	85.0	
7— 2—C —3—10	.606	−.080	.686		230.0	.658	.313			
SPECIAL DEVICES—HONEYCOMB										
3— 2—0 —3—0	0.864	−0.049	0.913	0.1908	72.0		0.461	63.0	66.0	
3— 2—C —3—0	.775	−.063	.838		239.0	0.684	.609	69.0	73.0	
7— 2—0 —3—0	.871	−.043	.914	.1908	72.0		.464	64.0	65.0	
7— 2—B_x—3—0	.844	−.048	.892		232.0	.664	.495	84.0	70.0	
AUXILIARY AIRFOIL										
7— 2—0 —3—0	0.961	−0.036	0.997	0.2200	83.0		0.386			No. 1 position 1.
7— 2—B_x—3—0	.906	−.039	.945		228.0	0.653	.475			Do.
7— 2—0 —3—0	.965	−.038	1.003	.2320	87.5		.351	86.0	63.0	No. 1 position 2.
7— 2—B_x—3—0	.876	−.045	.921		225.0	.646	.423	82.0	64.0	Do.
7— 2—0 —3—0	.977	−.028	1.005	.2040	77.0		.458			No. 2 position 1.
7— 2—B_x—3—0	.905	−.038	.943		229.0	.657	.493			Do.
TAIL PUMP CONDUCTIVITY 0.0250										
19— 5—0 —3—0				0.1087	41.0		0			Zero cooling air.
2— 5—0 —3—0	0.928	0.357	0.571	.1272	48.0		.685			
2— 5—B —3—0	.903	.281	.622		242.0	0.693	.270			
NACELLE 1—BAFFLES BACK ½ INCH—CONDUCTIVITY 0.0909										
7— 2—0 —3—0	0.992	0.116	0.876	0.2000	75.5		0.837	68.0	72.0	
7— 2—B_x—3—0	.891	.119	.772		229.0	0.656	.777	80.0	90.0	
7— 3—0 —3—0	.941	.588	.353	.1510	57.0		.480	89.0	98.0	
7— 6—0 —3—0	.999	−.139	1.138	.2910	110.0		.615	59.0	63.0	
7— 7—0 —3—0	.987	−.206	1.193	.4130	156.0		.393	60.0	63.0	
NACELLE 1—BAFFLES REMOVED—CONDUCTIVITY APPROXIMATELY 0.3–0.6										
0— 0—0 —2—0				0.399	150.5					
1— 2—0 —2—0	0.958	0.835	0.123	.1630	61.5			58.0	89.0	
1— 2—C —2—0	.878	.816	.062		243.0	0.697		65.0	113.0	
3— 2—0 —2—0	.909	.428	.481	.2040	77.0			38.5	87.0	
3— 2—C —2—0	.747	.320	.427		219.0	.628		42.0	95.0	
7— 2—0 —2—0	1.015	.768	.247	.1616	61.0			50.0	100.0	
7— 2—C —2—0	.868	.676	.192		237.0	.680		53.0	115.0	
7— 3—0 —2—0	.993	.902	.091	.1325	50.0			76.0	146.0	
7— 6—0 —2—0	.999	.447	.552	.2400	90.5			44.0	72.0	
BUMPED COWLING										
17— 0—0 —2—0	0.916	0.866	0.050	0.1259	47.5					
17— 0—C —2—0	.865	.800	.065		250.0	0.716				
17—10—0 —2—0				.1232	46.5					Nose closed off.
17—10—C —2—0					255.0	.730				Do.

TABLE I.—CONDENSED EXPERIMENTAL RESULTS—Continued

1	2	3	4	5	6	7	8	9	10	Remarks
Designation of arrangement (Nose / Skirt / Propeller / Inner cowling / Spinner)	p_f/q	p_r/q	(2−3) $\Delta p/q$	C_D (D/qF)	Drag in lb. at q=25.6 lb. per sq. ft., or thrust at $1/\sqrt{P_c}$=1.8 and q=25.6 lb. per sq. ft.	η_n at $1/\sqrt{P_c}$=1.8	η_p	Index temperatures: Front T_f	Index temperatures: Rear T_r	
NACELLE 2—STANDARD BAFFLES—CONDUCTIVITY 0.0424										
19— 9—0 —6—0				0.1126	42.5					Zero air.
7— 7—0 —4—0	0.962	−0.205	1.167	.2680	101.0		0.339	80.0	53.0	
7— 7—B_x—4—0	.889	−.256	1.145		208.0	0.595	.384	91.0	67.0	
7— 7—C —4—0	.886	−.241	1.127		205.0	.587	.357			
7— 6—0 —5—0	.967	.082	.885	.1696	64.0		.602	59.0	87.0	1.7-inch opening.
7— 6—B_x—5—0	.878	.075	.803		236.0	.677	.508	98.0	74.0	
7— 6—0 —5—0	.973	.026	.947	.1762	66.5		.597	83.0	57.0	2.5-inch opening.
7— 6—B_x—5—0	.892	.023	.869		234.0	.671	.522	100.0	75.0	
7— 6—0 —5—0	.959	−.029	.988	.1855	70.0		.562			3.9-inch opening.
7— 6—B_x—5—0	.881	−.033	.914		233.0	.668	.543			
7— 0—0 —5—0	.963	−.139	1.102	.2070	78.0		.510			
7— 6—0 —6—0	.982	.028	.954	.1749	66.0		.617			1⅞-inch rear opening.
7— 6—B_x—6—0	.877	.024	.853		237.0	.679	.574			
7— 6—0 —6—0	.993	.147	.846	.1630	61.5		.635			1¼-inch rear opening.
7— 6—B_x—6—0	.885	.134	.751		241.0	.692	.599			
7— 8—0 —6—0	.953	−.282	1.235	.4480	169.0		.172			2-inch flare.
7— 8—B_x—6—0	.872	−.425	1.297		156.0	.447	.230			Do.
7— 9—0 —6—0	.900			.1193	45.0					
7— 9—C —6—0	.890				251.0	.720				
SPINNERS										
7— 9—C —6—1	0.523				249.0	0.713				Position 1.
7— 9—C —6—1	.312				241.0	.691				Position 3.
7— 9—C —6—1	.257				237.0	.679				Position 4.
NACELLE 2—BAFFLES BACK ½ INCH—CONDUCTIVITY 0.0909										
7— 6—0 —5—0	0.983	0.428	0.555	0.1537	58.0		0.885	83.0	92.0	1¼-inch rear gap.
7— 6—0 —5—0	.979	.191	.788	.1755	67.0		.990	77.0	84.0	2¾-inch rear gap.
7— 6—0 —6—0	.980	.394	.586	.1590	60.0		.851	80.0	88.0	1¼-inch rear gap.
7— 6—0 —6—0	.975	.240	.735	.1735	65.5		.919	67.0	72.0	2-inch rear gap.
7— 6—B_x—6—0	.869	.241	.628		238.0	0.631	.804	89.0	97.0	Do.
7— 6—0 —6—0	.986	.151	.835	.1881	71.0		.900	66.0	73.0	2¾-inch rear gap.

TABLE II.—FRONT CYLINDER TEMPERATURES OBTAINED WITH VARIOUS SPINNERS

Designation of arrangement (Nose / Skirt / Propeller / Inner cowling / Spinner)	Front cylinder temperature T_f (°F.)	Ratio of front to rear cylinder temperature $\frac{T_f}{T_r}$	Remarks
1—2—C—3—9	83	1.106	
2—2—0—3—3	84	1.50	Dishpan behind propeller.
2—2—C—3—3	78	1.323	Do.
7—2—0—3—1	72.5	1.098	Position 1.
7—2—B—3—1	59	.952	Do.
7—2—C—3—1	65	1.033	Do.
7—2—B—3—2	67	1.032	
7—2—C—3—2	62	1.05	
7—2—0—3—3	112	.709	
7—2—B—3—3	50	.642	
7—2—C—3—3	68	.607	
7—2—C—3—3	82	1.322	Dishpan behind propeller.
7—2—C—3—2 & 3			
7—2—B—3—2 & 3	65	.663	
7—2—0—3—6	69.5	.939	
7—2—B—3—6	55	.873	
7—2—C—3—6	66	.892	
7—2—0—3—7	80	1.193	
7—2—C—3—7	65	1.202	
7—2—C—3—9	55	.647	

U. S. GOVERNMENT PRINTING OFFICE: 1937

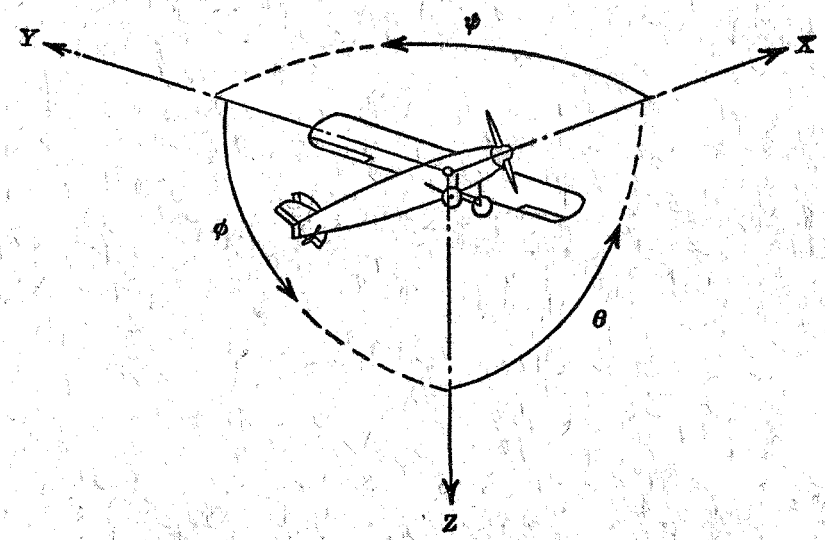

Positive directions of axes and angles (forces and moments) are shown by arrows

Axis		Force (parallel to axis) symbol	Moment about axis			Angle		Velocities	
Designation	Symbol		Designation	Symbol	Positive direction	Designation	Symbol	Linear (component along axis)	Angular
Longitudinal	X	X	Rolling	L	$Y \longrightarrow Z$	Roll	ϕ	u	p
Lateral	Y	Y	Pitching	M	$Z \longrightarrow X$	Pitch	θ	v	q
Normal	Z	Z	Yawing	N	$X \longrightarrow Y$	Yaw	ψ	w	r

Absolute coefficients of moment

$C_l = \frac{L}{qbS}$ (rolling) $\quad C_m = \frac{M}{qcS}$ (pitching) $\quad C_n = \frac{N}{qbS}$ (yawing)

Angle of set of control surface (relative to neutral position), δ. (Indicate surface by proper subscript.)

4. PROPELLER SYMBOLS

D, Diameter

p, Geometric pitch

p/D, Pitch ratio

V', Inflow velocity

V_s, Slipstream velocity

T, Thrust, absolute coefficient $C_T = \frac{T}{\rho n^2 D^4}$

Q, Torque, absolute coefficient $C_Q = \frac{Q}{\rho n^2 D^5}$

P, Power, absolute coefficient $C_P = \frac{P}{\rho n^3 D^5}$

C_s, Speed-power coefficient $= \sqrt[5]{\frac{\rho V^5}{P n^2}}$

η, Efficiency

n, Revolutions per second, r.p.s.

Φ, Effective helix angle $= \tan^{-1}\left(\frac{V}{2\pi r n}\right)$

5. NUMERICAL RELATIONS

1 hp.=76.04 kg-m/s=550 ft-lb./sec.
1 metric horsepower=1.0132 hp.
1 m.p.h.=0.4470 m.p.s.
1 m.p.s.=2.2369 m.p.h.

1 lb.=0.4536 kg.
1 kg=2.2046 lb.
1 mi.=1,609.35 m=5,280 ft.
1 m=3.2808 ft.